

Document downloaded from:

<http://hdl.handle.net/10251/202034>

This paper must be cited as:

Martí-Centelles, V.; Mcclenaghan, ND. (2022). Other Photoactive Inorganic Supramolecular Systems: Self-Assembly and Intercomponent Processes. En Springer Handbook of Inorganic Photochemistry 2022. Springer Link. 733-763. https://doi.org/10.1007/978-3-030-63713-2_26



The final publication is available at

Copyright Springer Link

Additional Information

This is an Author's Original Manuscript of a Book Chapter published by Springer in Springer Handbook of Inorganic Photochemistry on 26 June 2022, available at DOI: https://doi.org/10.1007/978-3-030-63713-2_26 ISBN: 978-3-030-63712-5

Vicente Martí-Centelles, Nathan D. McClenaghan (2022). Other Photoactive Inorganic Supramolecular Systems: Self-Assembly and Intercomponent Processes. In: Bahnemann, D., Patrocinio, A.O.T. (eds) Springer Handbook of Inorganic Photochemistry. Springer Handbooks. Springer, Cham. https://doi.org/10.1007/978-3-030-63713-2_26

5. Other photoactive inorganic supramolecular systems: Self-assembly and intercomponent processes

Vicente Martí-Centelles and Nathan D. McClenaghan

Institut des Sciences Moléculaires, Université de Bordeaux / CNRS, 351 cours de la Libération, 33405 Talence, France.

Table of Contents

| | | |
|-------|--|------|
| 5.1 | Abstract | p.2 |
| 5.2 | Introduction | p.2 |
| 5.3 | Intermolecular recognition and assemblies | p.4 |
| 5.3.2 | Soft matter / gels | p.8 |
| 5.3.3 | Mechanochromism and Aggregation-Induced Emission | p.12 |
| 5.4 | Intercomponent electronic energy and electron transfer processes | p.15 |
| 5.4.1 | Electronic energy transfer in supramolecular systems | p.23 |
| 5.4.1 | Reversible Electronic Energy Transfer | p.26 |
| 5.4.2 | Photoinduced Electron Transfer | p.28 |
| 5.5 | Other photoactive multicomponent systems and approaches | p.33 |
| 5.6 | Conclusion | p.33 |
| | List of abbreviations | p.34 |
| | References | p.36 |

5.1 Abstract

An overview of a range of topics in inorganic supramolecular photochemistry is presented, which are complementary to other chapters in this section, with particular emphasis on interacting discrete molecular species. These topics include non-covalent assemblies and interactions of photoactive molecules and the consequence of interaction on their properties. Photoinduced processes in supramolecular systems are considered, notably energy (uni- and bidirectional) and electron transfer, which are of particular relevance in the understanding biological processes or in new manifestations of photoinduced charge separation in the framework of artificial photosynthesis and smart materials. Other topics briefly discussed include mechanochromism, aggregation induced emission and supramolecular transfer of chirality.

5.2 Introduction

Supramolecular chemistry is generally considered as “chemistry beyond the molecule”, a definition forwarded by one of the founders of the domain, J.-M. Lehn in his seminal book.[1] From this perspective, supramolecular chemistry focuses largely on weak non-covalent interactions between molecules (or intramolecular interactions within a large molecule giving secondary structure, for example in defining protein conformations). Interactions may be specific, for example molecular recognition harnessing complementary hydrogen-bonding motifs or non-specific interactions such as van der Waals or electrostatic interactions. For the most part, electrostatic contributions are pre-eminent in most types of supramolecular interactions.[2]

However, considering supramolecular photochemistry, while the above definitions are clearly still valid, V. Balzani highlighted that a system may further be considered supramolecular if it is possible to split it into its individual subcomponents, where each of which retains their specific properties.[3,4] This evokes function arising from interaction of discrete, but linked, components. He pointed out that the distinction between large molecules and supramolecular species can be based on the degree of interaction between the electronic subsystems of the component units. Furthermore, when the interaction energy between subunits is small compared to other relevant energy parameters, the system can be defined as a supramolecular species. Thus, to some extent, supramolecular photochemistry may be considered as chemistry beyond the chromophore.

Indeed, light-driven processes can instil apparent intercomponent interactions, for example processes such as photoinduced electron transfer or electronic energy transfer, changing

reactivity and optical properties (as developed in section 5.4). Equally, ground state interactions can modify observed optical properties, being the functional basis for chemosensors and certain luminescent materials. The main outcome of supramolecular interactions on the excited state arise through changes of emission intensity (quantum yield), excited-state (and hence luminescence) lifetime and colour, as well as modulating redox properties and reactivity, which is of paramount importance in catalysis. Figure 1 schematically illustrates some major areas of inorganic supramolecular photochemistry.

Both the cases of intercomponent transfer and more classical non-covalent supramolecular interactions will be considered in the current chapter as it pertains to inorganic photochemistry. This chapter may be considered non-exhaustive and complementary to the detailed chapters in this supramolecular section, which deals with catenanes, rotaxanes, coordination cages and polymers, weak coordinative bonds, metal organic frameworks and lanthanide complexes. One aim is to highlight the current state of the art and processes with key examples and promising future directions in the area of supramolecular inorganic photochemistry. While traditionally less studied than their organic counterparts, inorganic systems are becoming increasingly more important, with the wide palette of available metal ions with specific coordination environments and conferring structural roles and excited-state properties to inorganic systems, being complementary to organic variants.

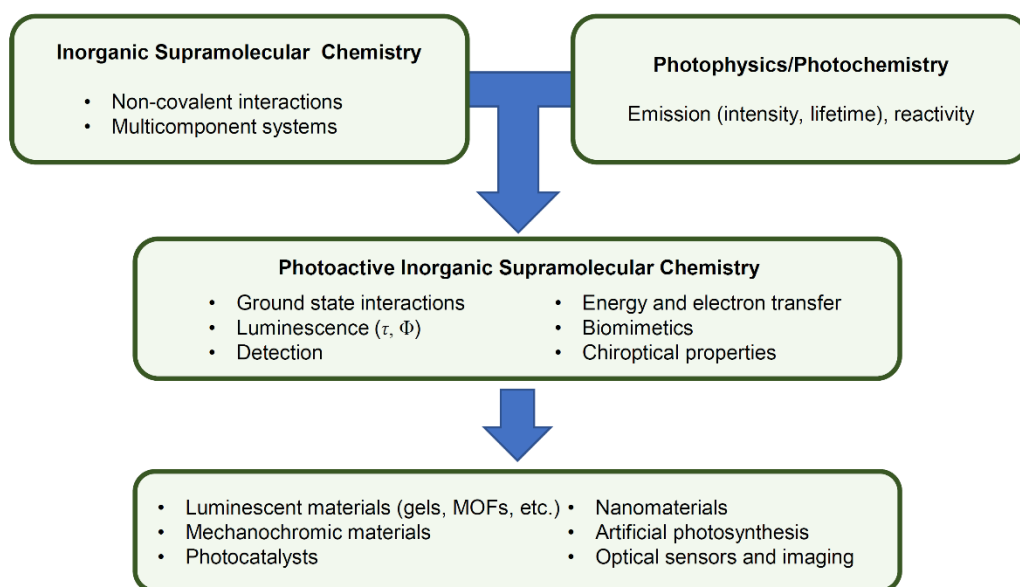


Figure 1. Scheme showing the scope of inorganic supramolecular photochemistry.

5.3 Intermolecular recognition and assemblies

In Nature, weak and reversible supramolecular interactions such as hydrogen-bonding, van de Waals, dispersion forces, hydrophobic effects, as well as ion binding play key roles in determining structure and function.[5] The concept of multivalency is also important, for example concerning protein-carbohydrate interactions.[6] In this section, some consequences of supramolecular interactions in photoactive inorganic systems are shown in terms of molecular recognition and materials development.

5.3.1 Molecular recognition between discrete molecules

Watson-Crick type pairing of complementary hydrogen-bonding groups (deemed donor and acceptor) offers a selective and directional means to introduce supramolecular interactions with metal complexes.[7,8] Indeed, when specific sequences of hydrogen-bonds are present this augments both the strength and selectivity of association between complementary sequences.

The effects of such association has been studied on interfacing inorganic chromophores with quenchers.[9] Figure 2 shows a selection of hydrogen-bonding dyads based on transition metal complexes as well as metalloporphyrins. Interporphyrin electron transfer was measured following photoexcitation within complex **1**, whose intercomponent bridge comprised a doubly hydrogen-bonding carboxylic acid bridge, and was compared to a covalent analogue (where the bridge comprises a fused dicyclopentane group which replaced the double carboxylic acid). Electron transfer from the Zn(II) porphyrin donor to the iron (II) acceptor was found to be $8.1 \times 10^9 \text{ s}^{-1}$ and importantly circa two times faster than the covalent analogue.[10] This points to the active participation of hydrogen-bonds in mediating processes such as electron transfer, clearly of consequence in biological systems. Transition metal polypyridine complexes **2a-2d** grafted with bases present in nucleic acids giving rise to the possibility of association via three hydrogen-bonds. Variants comprising luminescent Ru(II) or Os(II) tris-bipyridyl cores along with nucleobases adenine, thymine, cytosine or guanine could be assembled in order to investigate electronic energy transfer (EET, e.g. **2a – 2d**).[11] Indeed the lower lying triplet Metal-to-Ligand Charge Transfer ($^3\text{MLCT}$) level of $\text{Os}(\text{bpy})_3^{2+}$ (bpy=2,2'-bipyridine) is an effective energy acceptor for an excited $\text{Ru}(\text{bpy})_3^{2+}$ donor.[12,13]

While two point H-bonding between **2a** and **2c** was particularly weak at low concentration, the matched pair **2b** and **2d**, with the triple cytosine–guanine hydrogen-bond gave an elevated association constant ($6000 \text{ dm}^3 \text{ mol}^{-1}$ in CH_2Cl_2), allowing studies of intercomplex EET.

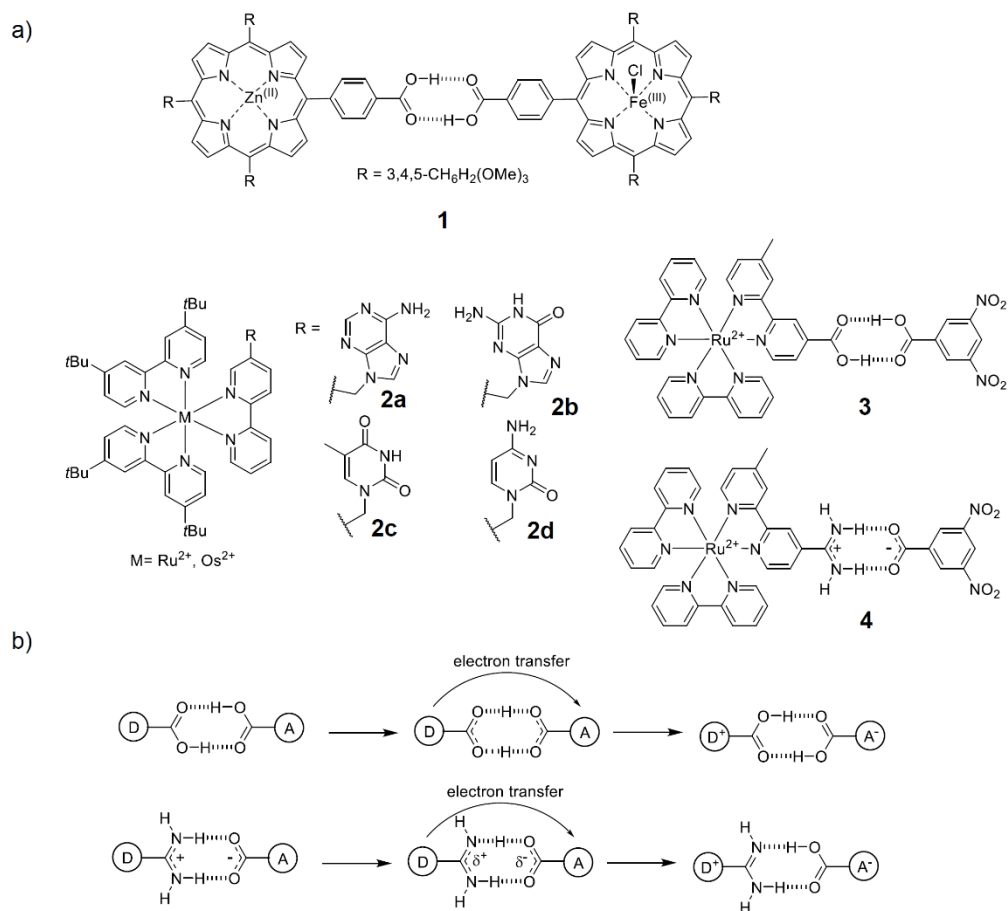


Figure 2. a) Binary hydrogen-bonding complexes; b) Non-covalent bridge assisted electron transfer.

Proton Coupled Electron Transfer (PCET) can be considered a bio-inspired means to promote electron transfer, and the two are often intimately linked.[14-16] In natural photosynthesis, light absorption results in a charge-separation process, resulting in an electron on one side of the membrane and a positive hole on the other. The electron reduces NADP⁺ to NADPH, a process that necessitates protons. The hole ultimately oxidizes water to O₂ on the other side of the membrane, which liberates protons. The resulting proton imbalance generates a thermodynamic gradient, which is the driving force for production of adenosine triphosphate (ATP). Clearly H-bonding protic functional groups can have a key role to play in this.

A few structurally simple complexes (**3** and **4**) were reported to investigate the coupled proton and electron transfer following photoexcitation.[17-21] Complex **3** featured a double hydrogen-bonded bridge with two carboxylic acid groups linking the inorganic electron donor and dinitrobenzene electron acceptor. In complex **4** the bridge linking a similar acceptor component comprised a protonated amidinium group associated with a deprotonated carboxylate.[17]

Faster photoinduced electron transfer was observed in **3** *c.f.* **4**, despite a lower anticipated driving force. This was ascribed to the symmetrical nature of a double proton transfer in the bridge, resulting in no net charge redistribution pending electron transfer, which would necessitate solvent reorganisation. Meanwhile, proton transfer in **4** results in a charge redistribution in the bridge, Figure 2b, which in turn would require changes in solvation. This is responsible for an activation energy barrier on the proton transfer process and therefore, electron transfer is slowed as the two processes are intimately associated. Furthermore, a kinetic isotope effect was shown, as replacing H atoms in the hydrogen-bonded bridges of **3** and **4** by D atoms slows down electron transfer by a factor of about 1.4 in each case. This means that cleavage of the O–D bond (for **3**) or the N–D bond (for **4**) is involved in the rate-determining step. Should no proton movement occur in concert with electron transfer, then the substitution of H for D would not affect the rates.

Clearly ground state supramolecular interactions can affect the observed optical properties, either directly or indirectly.[22-24] A direct effect would correspond to a situation where guest/analyte binding would lead to a shifted HOMO-LUMO gap and consequently would be manifested by a spectral shift / change in colour. This is the basis for colorimetric sensors, which have proved successful in “naked eye” detection of several strong binding inorganic species including mercury and fluoride.[25-26] The generic principle for guest-induced colour modification is presented in Figure 3a. The dye comprises an electron donor-moiety linked to an electron acceptor by a π -conjugated bridge, and as such is highly polar. This is particularly true upon photoexcitation due to enhanced charge transfer and, as a result, such dyes are referred to as Internal Charge Transfer (ICT) or Photoinduced Charge Transfer (PCT) dyes. Sensitivity and selectivity is provided by a receptor group which is integrated either at the donor or acceptor terminus of the chromophore. If integrated at the latter, binding a cation for example would result in a stabilisation of the excited state with a resultant red-shifted spectrum (e.g. coumarin-comprising **5**), while an opposite effect would be observed if the receptor were integrated at the donor terminus. Equally, modifications in luminescence mirroring absorption changes would be expected (when the ion is not expelled during the excited-state lifetime). Differing emission quantum yields may be anticipated between the complexed and uncomplexed forms.

Optical detection of metal cations can be arranged in a rather straightforward way and is of particular importance in detection and quantification of heavy metal water pollution, for example. Perhaps more challenging is anion sensing, which is rapidly becoming a mature field.[27] Figure 3b shows some examples (**6** and **7**) where the luminescence of transition metal complex receptors is quenched by interacting with anions.[28,29]

Indirect methods can include blocking an intramolecular process such as energy and/or energy transfer (described in a later section) or bond cleavage/insertion to change a dye structure and resultant optical properties. Various metal-driven chemical cleavage reactions, such as metal-promoted hydrolysis, metal-induced desulfurization followed by hydrolysis, and metal-induced deprotection, have been utilized for the development of chromogenic and fluorogenic probes for metal ions. **8** is an example where AgI formation and subsequent irreversible tandem ring-opening and formation processes conspire to develop a rhodamine-based probe **8** for Ag⁺ in

aqueous ethanolic solution (20%) (Figure 3c).[30] The probe shows a linear fluorescence response to Ag^+ in the range of 0.1–50 μM with a detection limit of 1.4×10^{-8} M. Equally, utilisation of the probe to quantify silver nanoparticles in consumer products was described, following the oxidation of silver nanoparticles to Ag^+ by hydrogen peroxide.

Compound **9** was reported as a fluorescent probe for H_2O_2 assay (detection limit, 3.2 μM).[31] This probe has an iron complexing moiety as a reaction site for H_2O_2 and a 3,7-dihydroxyphenoxazine fluorescent reporter unit. Reaction of **9** with H_2O_2 leads to the release of fluorescent resorufin (Figure 3d). As compared to many of other H_2O_2 probes, this reaction is selective for H_2O_2 and can eliminate the interference from phenol derivatives. Optical detection of reactive oxygen species (ROS) and reactive nitrogen species (RNS) is particularly difficult not least because of their transient nature but is a developing field due to the importance of these species in biology.

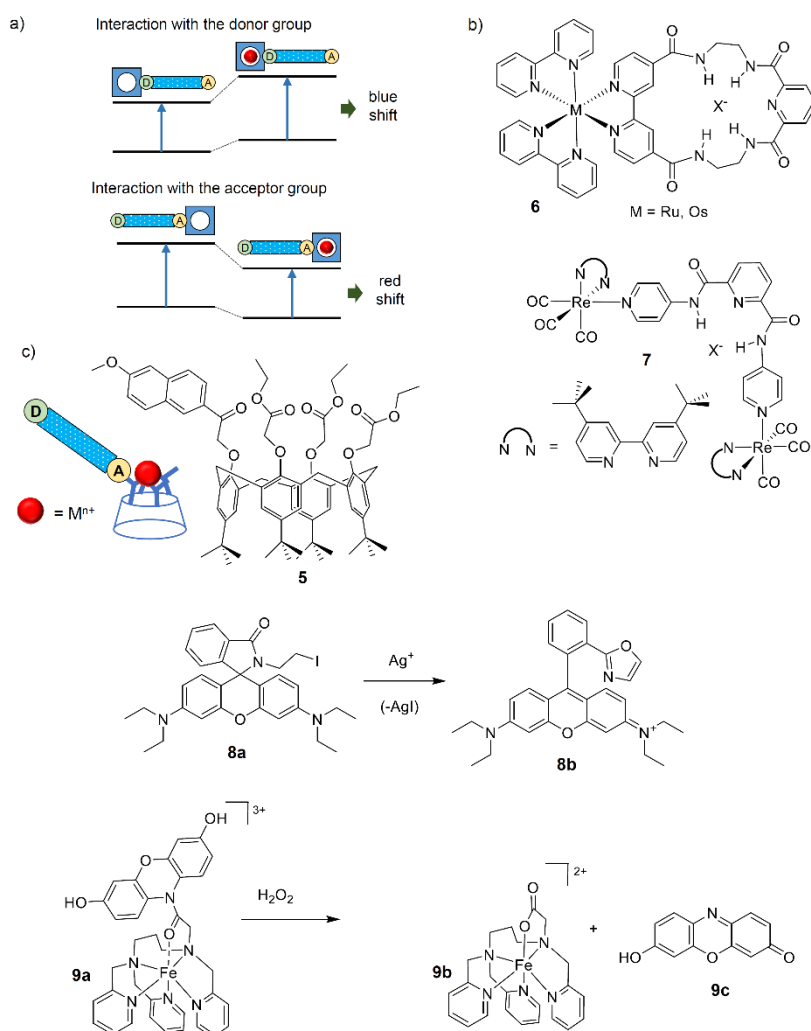


Figure 3. a) Photoinduced Charge Transfer (PCT) dyes and interaction with metal ions; b) Luminescent anion sensors; c) Ion sensing through bond cleavage; d) Inorganic sensor of reactive oxygen species H_2O_2 .

5.3.2 Soft matter / gels

Going beyond supramolecular complexes of low molecularity (such as 1:1 host: guest systems) leads to the idea of molecular assemblies and self-assembled materials. Supramolecular self-assembly involves arrangement of smaller entities into more organized systems, harnessing reversible dynamic interactions using chemically encoded information.[32-35]

To obtain such assemblies, in addition to the supramolecular interactions cited above, metal-metal interactions can be evoked in certain inorganic species, which can effectively modify the electronic and optical properties as well as providing a structure-directing role.

To rationalize the photophysical behaviour of complexes and aggregates, firstly we shall consider frontier orbitals via molecular orbital diagrams for a generic transition metal complex and associated transitions then expand the discussion to square planar d^8 compounds which have a tendency to aggregate (Figure 4a vs 4b).[36]

Globally photophysical properties of closed-shell complexes with unsaturated ligands are largely derived from the presence of filled molecular orbitals with strong metal d character as well as of low-lying empty, anti-bonding π^* orbitals located on the ligands of similar energy. Energetic proximity of different electronic states and their different nature is noted as well as spin-orbit coupling exerted by the presence of heavy atoms which allows mixing of the singlet and triplet manifolds. Indeed, spin-orbit coupling is related to the fourth power of the atomic number Z ($SOC \propto Z^4$), leading to fast intersystem crossing ISC processes (often sub-picosecond) between electronic excited states of different multiplicity (i.e. singlet and triplet). Spin-orbit coupling is considered to relax the spin selection rules promoting efficient radiative decay pathways from the lowest-lying excited state with mainly triplet character (T_1) to the singlet ground state (S_0), i.e. phosphorescence. Thermal relaxation of the excited molecule to its fundamental vibrational state within the T_1 electronic state gives rise to the typically observed large Stokes shift in luminescence derived from transition metal complexes. Radiative deactivation channels occur between states with mixed spin character, is responsible for the relatively slow excited state deactivation kinetics, which typically falls on the 100s of nanoseconds to 10s of microsecond time scale. Photoexcitation of such compounds (UV-vis) region leads to the formation of excited states with a different electron density distribution considered as metal centred (MC), ligand centred (LC), interligand or ligand-to-ligand charge transfer (ILCT or LLCT), ligand-to-metal charge transfer (LMCT) and metal-to-ligand charge transfer (MLCT) (Figure 4a). The aforementioned description considers both d^6 and d^8 complexes with appropriate ligands.

The square-planar geometry of d^8 transition metal complexes, imparts a strong tendency to stack, through ground-state weak intermolecular metal-metal and/or ligand-ligand interactions through the π -electron cloud of the aromatic rings. Platinum (II) complexes being the more widely studied d^8 metal complex will be the primary focus of our attention although other related metals will also be considered.[37-46]

Figure 4b shows the diagram of pertinent molecular orbitals (MOs) for both monomeric and also for two axially interacting platinum complexes. Typically the highest occupied and lowest unoccupied molecular orbitals, respectively the HOMO and LUMO, of platinum compounds have d_{xy} and d_{xy}^* character when cyclometalating ligands provide a strong field in conjunction with good π -accepting properties. For a metal centre having a square-planar arrangement of the coordinating ligands, ligand field theory predicts relaxation of degeneracy of the d orbitals and a filled d_{z^2} orbital orthogonal to the molecular plane, which interacts minimally with the ligand coordination sphere, and lies below the HOMO level in energy. The occupied d_{z^2} orbital is thus free to interact with neighbouring solvent molecules or other platinum complexes. In the second scenario, the formation of ground-state metallophilic interactions ($d_{z^2}-d_{z^2}$), destabilizes the filled d_{z^2} orbitals, resulting in a modification of the character of the HOMO level from d_{xy} to d_{xy}^* .

As a result of the Pt-Pt interaction, new excited states are therefore available such as metal-metal-to-ligand charge transfer, namely MMLCT ($d_{xy}^*-d_{xy}^*$), as revealed in Figure 4b. Interestingly, these charge transfer states typically show absorption and luminescence that are significantly red-shifted with respect to the parent platinum complexes. The energy of such charge transfer transitions, and degree of red-shifting, depends strongly on the metal-metal distance, with the electronic interaction becoming significant at a distance typically below 3.5 Å.

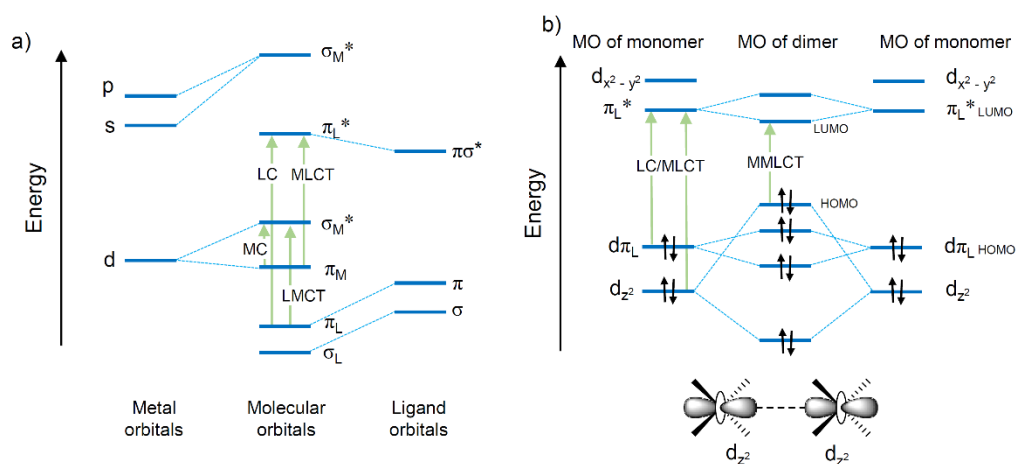


Figure 4. (a) Molecular Orbital (MO) diagram for a generic transition metal complex and relative spectroscopic excitation transitions; (b) MO diagram of two interacting square-planar platinum(II) complexes, showing the intermolecular d_{z^2} orbital overlap in the ground-state dimer.

In organic or aqueous media, luminescent Pt(II) complexes are able to form homo-[47-48] and heterometallic [49-51] supramolecular architectures and superstructures such as nanowires,[52] nanosheets, nanowheels, nanotubes,[53] liquid crystals,[54] and metallologs formed from low molecular weight gelators.[55-57]

For the most part, organoplatinum(II) gelator complexes comprise ligands with N donor ligands, and a novel series of phosphine-containing platinum(II) alkynyl oligomers with various π -conjugated and rigid linkers **10a–10c** was reported.[58] The metallo gels showed significantly blue shifted absorption and emission, indicative of exciton interactions resulting from H-aggregates of platinum(II) chromophore. Upon integrating chiral moieties into the central rigid core (**10c**), a strong circular dichroism (CD) signal was observed in the dodecane gels. Mixed gels of **10a** and **10b** gave rise to triplet energy transfer from **10a** to **10b** in the gel states (Figure 5, bottom), since the 1,4-phenylene core in **10a** could act as an electron donor while the 2,5-thienylene core in **10b** could act as an acceptor. Time-resolved emission studies are consistent with triplet exciton hopping in the aggregate resulting from Dexter exchange energy transfer (*vide infra*). A series of platinum(II) alkynyl complexes was recently reported with iptycene as the linker that showed excellent gel formation properties in common organic solvents.[59-60]

The aforementioned species can have very appealing (electro)optical,[61-63] sensing [64-65] and semiconducting properties.[66] Furthermore, the formation of such metallophilic interactions in luminescent square planar platinum complexes, and the subsequent modulation of their photophysical properties, can be induced by the presence of biologically relevant molecules and polyelectrolytes in aqueous media.[67-69]

The aggregation process of luminescent platinum complexes can be directly followed by confocal fluorescence microscopy when the luminescence spectrum is greatly shifted due to intermolecular interactions, including metal-metal interactions and face-to-face π -stacking, which modify the electronic properties.[61, 70] In one example, assembly of charge neutral mononuclear amphiphilic luminescent square-planar platinum(II) complexes (**11**) was recently shown to correspond to two kinetic assemblies and the more stable thermodynamic one, using different colour readout of the rapidly and more slowly forming species.[71] Indeed the weakly emitting blue monomer ($\Phi = \text{ca. } 1\%$), upon adding a dioxane solution of **11** to a 95:5 % dioxane-water mixture was shown to initially form a kinetic product – which was oxygen-insensitive orange emitting ($\Phi = 84\%$) spherical nanoparticles (126 nm diameter) resulting from metallophilic interactions. After three weeks ageing the thermodynamic product, micrometric ribbons lacking M-M and π - π interactions giving monomer-like emission (but with 20-fold emission increase). The evolution of the system was shown to be sensitive to solvent composition, in one case the initially drop-cast orange aggregates gave way to green aggregates, with elongated Pt-Pt distances in a face-to-face arrangement and ultimately to stable blue-emitting ribbons. It is noteworthy that this stable product can be photochemically reverted to the kinetic green intermediate. Size control of the aggregates was achieved by seeded growth under living supramolecular polymerization conditions. The authors highlight that controlling multiple supramolecular pathways will help in designing complex systems in and out of thermodynamic equilibrium.

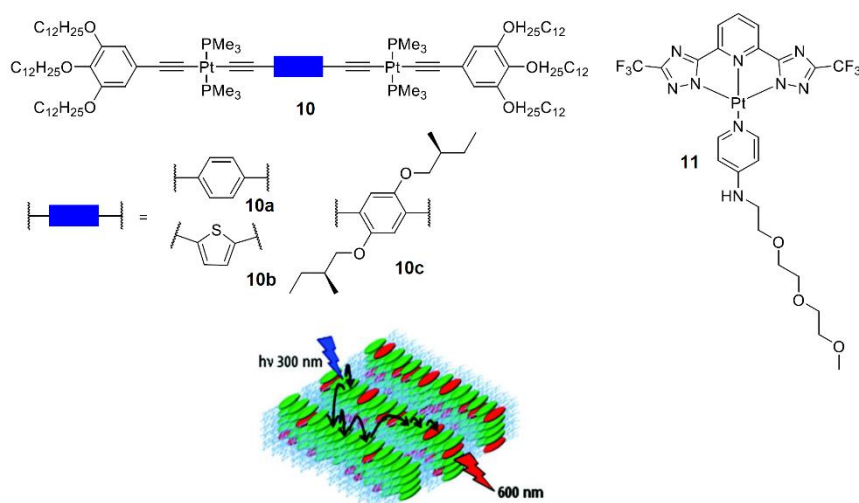


Figure 5. Top) Self-assembling Pt(II) complexes; Bottom) Representation of triplet energy migration in a material comprising **11**. Reproduced with permission from *J. Am. Chem. Soc.* **130**, 82535-82545 (2008).

In the area of biological imaging, while Pt(II) complexes have been extensively studied for cancer therapy,[72-74] only very few examples have shown potential for theranostic applications. However there are some advantageous properties that could be noted for Pt(II) complexes with respect to a highly demanding set of requisite properties for imaging biological media.[36] More precisely, i) the compounds ought to be both soluble and stable in aqueous media/phosphate buffered solution (PBS) and/or cell culture media. ii) In order to penetrate the cell it should have a sufficient hydrophobicity to cross the phospholipid cell membrane. iii) It should have low cytotoxicity and produce no toxic compounds (including reactive oxygen species (ROS)). iv) The chromophore should further be red-emitting, insensitive to oxygen and possess a high photochemical stability. v) The molecule should preferentially reside in specific organelles/ cell compartments. While point v) can be addressed by bioconjugation with specific targeting agents, Pt(II) complexes can correspond quite well to points i)-iv). Indeed the metal-metal interactions, can red-shift emission, while maintaining high photoluminescence quantum yields, protecting from oxygen-quenching and the environment ensuring a long-excited state lifetime. Long excited-state lifetimes are of interest for imaging dyes after the intrinsic background cellular fluorescence has decayed, using time-gated detection, which is available on essentially all modern fluorescence microscopes (*vide infra*).

The favourable properties cited above can also be associated with other metal complexes which are able to provide sizeable metallophilic interactions,[36] such as Au(I)-, Ag(I)-, Pd(II)-, Cu(I), Tl(I) and Hg(I)-based transition metal complexes.[75-82]

Gold(I) alkynyl complexes [83,84] are known to be among the most luminescent gold complexes, but the less-explored luminescent gold(III) complexes, in general, could be obtained by raising the d-d ligand field excited state energy via the coordination of good π -donor ligands. Homo-

and heterometallic gold(I) complexes that are not sterically hindered in structures often display weak intra/intermolecular Au–M interactions (M = heavy atoms including gold itself). These weak interactions usually play a crucial role in governing the photophysical properties, especially when the metal-based orbitals contribute significantly to the character of the frontier molecular orbitals.[77]

5.3.3 Mechanochromism and Aggregation-Induced Emission

Mechanochemistry offers a way of performing chemical reactions using mechanical forces as the energy input, however most of the reactions use energy in the form of heat, light or electricity. This is a less well-known way of providing energy to activate chemical species in “solvent-free” conditions and offers a way to perform reactions in the solid state. [85] In this regard, the mechanochromism produces a change in color as a result of applying external mechanical forces. Typically mechanochromic luminescent metal complexes change their solid-state emission spectra upon application of sufficient pressure or mechanical force (which may include grinding, crushing, rubbing and/or extrusion) and are an emerging class of compound of interest in the areas of luminescent switches, mechanosensors, mechanohistory indicators, security papers, optoelectronic devices and data storage.[86] Switching occurs through a chemical or physical structural change which affects the electronic structure (notably the HOMO-LUMO energy levels), the latter approach being considered more effective via shifting molecular arrangement, conformation and intermolecular interactions. Altering molecular packing to achieve dynamic control of highly efficient and reversible solid-state luminescence is more practical because of low pressure/force demand and high reversibility. While many mechanochromic organic variants are known based on organic dyes, liquid crystals, and polymers, inorganic variants offer an interesting and potentially richer alternative.[87-91] Such luminescent complexes comprise different metals and some representative examples based on Zn(II), Au(I), Pt(II) are shown in Figure 6, while there are equally noteworthy examples based on Ag(I), [92-93] Cu(I) [94-95], Al(III) [96] and Ir(III) complexes.[97]

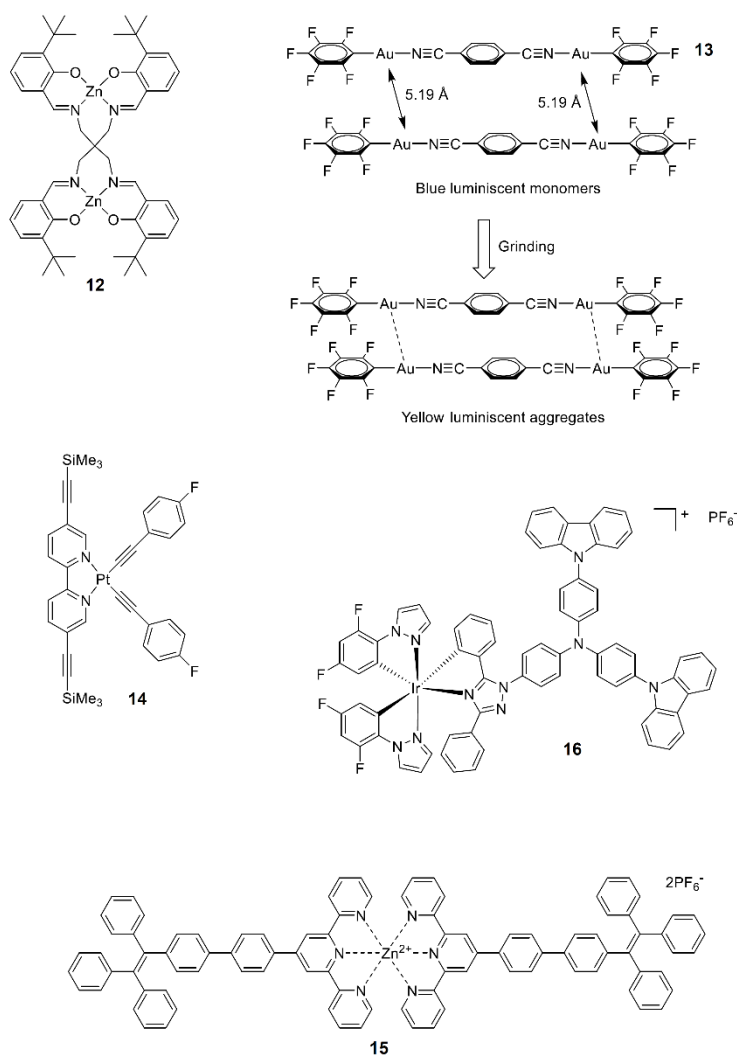


Figure 6. Complexes displaying solid-state mechanochromism (**12 – 14**) and aggregation-induced emission (**15 – 16**).

Figure 6 shows several molecules that exhibit solid-state mechanochromism. Helical 3,3'-di-tert-butyl-salen-zinc (II) complex **12**, whose fluorescence emission changes from green to longer-lived blue upon mechanical grinding. This is attributed to a crystal phase transition which weakens intermolecular π - π interactions.[98]

A gold(I) complex, [(C₆F₅Au)₂(m-1,4-diisocyanobenzene)] (**13**), which has a solid-state photoemission that can be reversibly switched by external stimuli, was reported.[99] Upon gentle grinding in a pestle and mortar, the blue luminescence changed to an intense yellow luminescence with a 118 nm spectral red-shift. Treatment of the ground powder with drops of dichloromethane, caused the yellow luminescence to revert to the original blue colour. The blue-to-yellow conversion achieved by subsequent regrinding can be repeated several times without causing any degradation in the luminescence. Grinding the microcrystalline powder is

proposed to produce an amorphous state having aurophilic interactions giving the longer wavelength emission. On the nanoscale this corresponds to shifting the Au-Au distance from 5.19 Å to the range 2.7-3.3 Å. Recovery involves dissolution and recrystallization induced by a volatile solvent. Replacing the central phenyl ring with methylated variants as well as biphenyl and extended organic bridges was seen to diminish or arrest the mechanochromic behaviour.[100] **14** is a square-planar bis(*s*-fluorophenylacetylide) Pt(II) complex which undergoes a yellow-orange to dark red luminescence change based on mechanochromism stimulus which is reversible upon exposure to acetone or shifted over 150 nm on exposure to chlorinated solvent vapours, which was rationalized via DFT calculations to be due to M-M interactions.[101]

Monomer **11** cited above equally demonstrated mechanochromism at the nanometer scale.[102] Mechanical manipulation of the long persistent blue fibres described above via AFM allowed some quantification of the nanoscale mechanochromism arising from static pressure (piezochromism) and shear-based mechanical stimuli (tribochromism) and compare with bulk pressure-dependent luminescence observed with diamond anvil cell (DAC) technique. An applied pressure of between 5 kbar and 25 kbar gave rise to mechanochromic effects. Due to the local nature on the mechanochromic effect, i.e. on going from the native to the “mechanically-stressed forms”, high density information (features inferior to a micron) writing with AFM nanolithography applied on individual self-assembled ribbons. Photochromism was also identified offering the possibility to erase written information.

Aggregation-induced emission (AIE) complexes harness the structural relationship between AIE complexes and mechanochromism, with more easily implemented AIE complexes potentially promising to play the role of mechanochromic luminescent complex surrogates. Globally, mechanochromic complexes are difficult to design as packing predictions and influence on solid-state properties such as emission are difficult to predict. However, incorporation of AIE-active groups such as triphenylethylene, tetraphenylethylene, silole, cyano distyrylbenzene, and distyrylanthracene derivatives in ligands were found to render complexes liable to exhibit mechanochromism.[87,103] Figure 6 shows two examples of complexes which undergo AIE due to the incorporation of specific organic ancillary aggregating agents. Complex **15** comprising a $Zn(tpy)_2^{2+}$ unit along with two peripheral tetraphenylethene groups, the latter rendering the complex AIE-active.[104] Various studies demonstrated that the grinding, heating, and solvent fuming-induced fluorescence changes can be achieved by tuning the molecular packing in the solid state. The variations in the emission wavelengths for the ligand and the complex before and after grinding were 38 nm and 81 nm, respectively, indicating that complexation may increase the wavelength variation range in mechanofluorochromism in certain cases. Upon exposure to acid and base vapours such as those of trifluoroacetic acid (TFA) and triethylamine (NEt_3), the fluorescence emissions and colours of these complexes exhibited an off/on switching effect. This work was thus reported a prototype metal ion complex that exhibits the AIE effect as well as multistimulus-responsive fluorescence features. Equally, luminescent transition metal complexes have been considered. Cationic **16** $[Ir(dfppz)_2(L)](PF_6)$, which contains 1-(2,4-difluorophenyl)-1H-pyrazole (dfppz) as the cyclometalating ligand and a dendritic carbazole-containing ancillary ligand. While non-emissive in solution, it displays enhanced emission in the

solid state. In addition, the as-prepared powder of **16** obtained through recrystallization exhibits a bright-yellow emission, which changes to orange upon grinding. Thus, **16** is a mechanochromic as well as an AIE-active material. Single-crystal analysis showed that the complex exhibits a distorted octahedral geometry around the Ir atom, which is coordinated by two cyclometalated ligands and one ancillary ligand. Close investigation of the molecular packing structure of **16** revealed that multiple intermolecular C–H/π interactions exist in its single-crystal structure. Given these weak interactions, the crystal structure of **16** can be easily interrupted. This change can be triggered through a packing rearrangement or a phase transition under external pressure.[105]

5.4 Intercomponent electronic energy and electron transfer processes

Both electronic energy transfer and electron transfer are widespread in natural and artificial chemical systems, while light provides both a trigger and probe that can be applied to study such processes with high spectral, temporal and spatial resolution. Supramolecular architectures offer a means to orient active components in terms of their mutual distance and orientation, both of which are key parameters in these transfer processes. Equally, the nature of the supramolecular interaction itself can be of fundamental importance and actively participate in the transfer. Owing to the importance of metal complexes in metalloproteins and redox enzymes, relatively high photostability and excellent redox processes in many cases, it is of little wonder that inorganic complexes represent an enduring area of research.

5.4.1 Electronic energy transfer in supramolecular systems

Electronic energy transfer has been widely studied in multicomponent systems and for more detail the reader is referred to the excellent reviews on the topic.[106-108] Equally in this handbook, chapters dealing with specific theoretical aspects are worthy of consultation. As such, herein we will only give a brief overview of key aspects illustrated with some examples with a particular focus on supramolecular systems. A major motivation for research in this domain is an attempt to reproduce and quantify aspects of photosynthesis and develop artificial photosynthetic systems. Indeed, in photosynthesis, following light absorption by a manifold of absorbing pigments the management of energy is important, notably rapidly funnelling it down to the special pair, where it is used to drive an important electron transfer process. This light harvesting is an important aspect of photosynthesis, and approaches to artificial photosynthesis.[109-111]

In this goal, several parameters are important to consider including conformation and distance in supramolecular systems, which thus considers intramolecular, intra-assembly processes and

factors including interactions with a second species/second sphere.[112] Bichromophoric dyads comprising an energy donor and an energy acceptor (equally subsequently referred to in the following sections as donor and acceptor and not to be confused with electron donors and acceptors) and represent convenient model systems to investigate both EET and PET in well-designed systems.[113-115] Such systems may be rigid or flexible, which is of major importance considering kinetic aspects. Here we will consider bichromophoric prototypes and move towards assemblies. To probe such transfer processes in photoactive systems steady-state and time-resolved fluorescence and time-resolved spectroscopies are of particular interest.

Considering conformation and distance, close approach of the energy acceptor to the donor fluorophore may lead to a diminished observed emission. The relationship between quenching efficiency and distance depends on the quenching mechanism. Here we will consider two energy transfer mechanisms which are pertinent for inorganic supramolecular systems, namely Förster Resonance Energy Transfer (FRET) and subsequently Dexter energy transfer.[116-123] FRET is largely insensitive to effects of the surrounding solvent and depends primarily on the distance between the donor and acceptor fluorophores. As such, FRET equates to a “spectroscopic ruler”.

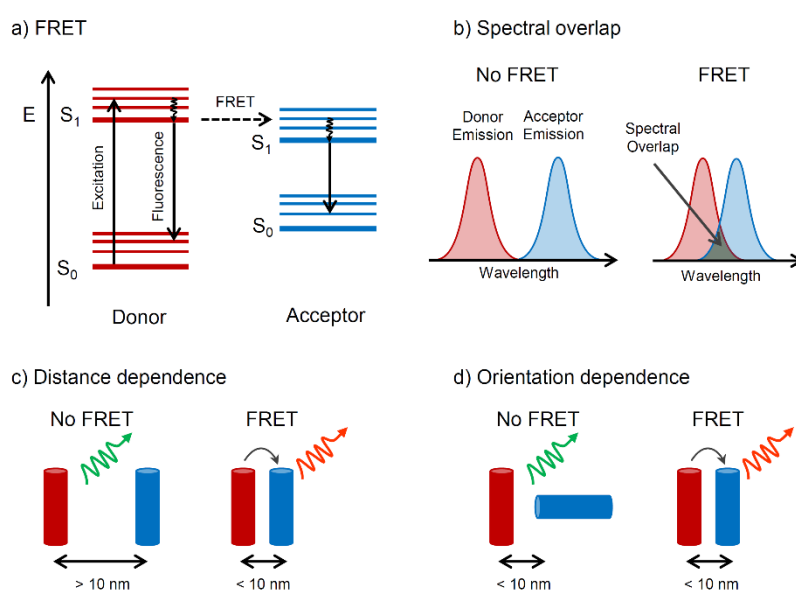


Figure 7. Key considerations for efficient Förster Resonance Energy Transfer (FRET) between donor and acceptor chromophores. a) Energy; b) Spectral overlap; c) Distance; d) Mutual chromophore orientation.

Equation 1 describes the rate of FRET at a distance (r), where energy is transferred in a non-radiative fashion from the donor to acceptor (quencher) moieties through long-range dipole-dipole interactions, thereby deexciting / quenching donor fluorescence and exciting/sensitizing emission of an acceptor fluorophore (see Figure 7a). Meanwhile R_0 , the Förster critical distance (the distance at which transfer and spontaneous decay of the excited donor are equally probable, i.e. $k_T = 1/\tau_D^0$) can be determined according to Equation 2 for a process in an

isotropic medium. Here, τ_D^0 is the unquenched excited-state lifetime of the donor, κ^2 is the orientational factor, which is 2/3 in free solution but can take values from 0 (perpendicular transition moments) to 4 (collinear transition moments), Φ_D^0 is the fluorescence quantum yield of the donor in the absence of transfer, n is the average refractive index of the medium in the wavelength range where spectral overlap occurs, $I_D(\lambda)$ is the fluorescence spectrum of the donor normalized such that $\int_0^\infty I_D(\lambda) d\lambda = 1$, $\varepsilon_A(\lambda)$ is the molar absorption coefficient of the acceptor (in $\text{dm}^3 \text{mol}^{-1} \text{cm}^{-1}$) and λ is the wavelength (nm).[120] Equally, as an alternative (or complement to) intensity changes, an increasingly popular method to determine FRET is to measure the fluorescence lifetime of the donor fluorophore in the presence and absence of the acceptor to gauge the degree of transfer quenching.

$$k_T = \frac{1}{\tau_D^0} \left[\frac{R_0}{r} \right]^6 \quad (\text{Eqn. 1})$$

$$R_0 = 0.2108 \left[K^2 \Phi_D^0 n^{-4} \int_0^\infty I_D(\lambda) \varepsilon_A(\lambda) \lambda^4 d\lambda \right]^{1/6} \quad (\text{Eqn. 2})$$

So the rate of FRET energy transfer depends largely upon the degree of spectral overlap between the donor emission and acceptor absorption spectra (see Figure 7b), the donor quantum yield, the distance between donor and acceptor molecules (see Figure 7c) and the relative orientation of the donor and acceptor transition dipole moments (see Figure 7d). Equation 3 allows us to estimate the efficiency (E) of FRET and observe nanometric approach of donor and acceptor units, either through the donor emission intensity (I_{DA} is the emission in the presence of an acceptor, I_D is the emission intensity in the absence of an acceptor; A_D and A_{DA} and donor and conjugate absorbances) or the emission lifetime (τ_{DA} is the emission lifetime in the presence of the acceptor, while τ_D is the intrinsic emission lifetime).

$$E = 1 - \frac{A_D I_{DA}}{A_{DA} I_D} = 1 - \frac{\tau_{DA}}{\tau_D} \quad (\text{Eqn. 3})$$

With the efficiency of the energy transfer process varying proportionally to the inverse sixth power of the distance separating the donor and acceptor components (Equation 1 and 2), FRET measurements allow the determination of distances when they are < 10 nm from each other (see Figure 7). Such operational distances mean FRET offers a means to study non-covalent interactions in both synthetic and biological supramolecular systems. Molecular forces, protein conformations and kinetics of assembling may be determined, and in vivo nanoparticle drug release may be observed.

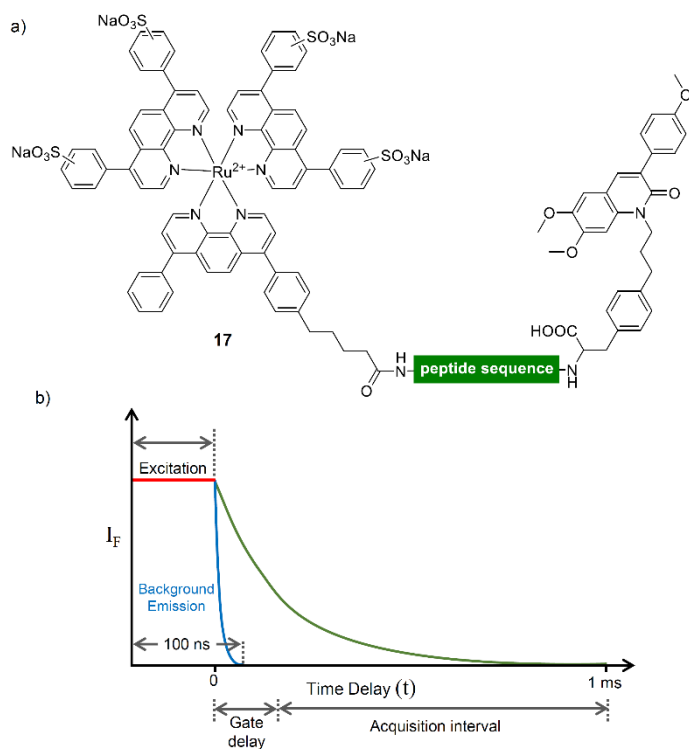


Figure 8. a) Example of FRET donor-acceptor dyad; b) Time-gated detection of emission.

Figure 8a shows an example of a FRET dyad (**17**) which can act as a ratiometric luminescent probe for the assay of enzyme activity, with the donor and acceptor dyes being connected through an enzymatically cleavable linker.[124] **17** comprises a carbostyryl moiety as the FRET donor and a ruthenium(II) bathophenanthroline complex as the FRET acceptor. Reaction of **17** with thrombin leads to the cleavage of the peptide sequence and thus the change of the luminescence intensity ratio of the donor and the acceptor at 420/618 nm. Additionally, with an ester bond, a phosphodiester bond, or the substrate structure of β -lactamase as a cleavable linker, FRET based ratiometric probes have been reported for monitoring the activity of esterase,[125] phosphodiesterase,[126,127] and β -lactamase.[128]

An interesting alternative to classic FRET dyads response is time-resolved fluorescence energy transfer (TR-FRET), which is the practical combination of time-resolved fluorometry (TRF) with Förster resonance energy transfer (FRET). This has proved particularly popular in biological assays, notably with inorganic complex-organic chromophore dyads. TR-FRET combines the low background aspect of time-gated luminescence with the homogeneous assay format of FRET. The resulting assay provides versatile, reliable and sensitive methodology in addition to higher throughput and fewer false positive/false negative results.[129,130] Figure 8b illustrates the advantage of using time-gated emission detection to obtain a clean signal free from contamination of background fluorescence or unsensitized acceptor emission, which can be easily implemented on modern commercial instruments. Thus TR-FRET probes provide an advantage over conventional FRET as the sensitized acceptor emission is distinguished from

energy donor and direct acceptor emission both in respect to spectral and to temporal characteristics.[131]

Lanthanide chelates, due to their line-type emissions and extremely long decay times, are ideal TR-FRET donor candidates.[132] The TR-FRET induced acceptor emission generally has a decay related directly to donor decay time and inversely to the energy transfer efficiency. In most of the applications, the relatively long distance e.g. in protein–protein complexes results in low energy transfer efficiency, and hence, relatively long decay time, typically in the range of 100–1000 μ s. Such a FRET signal is easily detected with commercially-available time-resolving plate fluorimeters based on gated detection. The TR-FRET signal is distinguished from background and from directly-excited acceptor emission by temporal filtering and from the long decay donor by its red-shifted emission.

Luminescent europium(III) chelates are the most commonly used donors in TR-FRET, and are widely commercialized e.g. TRACE®/Kryptor® system of Brahms, HTRF® of CisBio International, LANCE® by Perkin-Elmer, and in LRET® of Amersham. The long decay time allows efficient dynamic energy transfer reactions with flexible complexes, and abates the orientational factor effect on FRET. The relatively long wavelength emission ensures low background for acceptor measurement (e.g. 665 nm). Allophycocyanin is the most commonly used energy acceptor with europium(III) chelates is, which due to its very high molar extinction coefficient ($700,000 \text{ M}^{-1} \cdot \text{cm}^{-1}$) and quantum yield (0.7) results in a long Förster radius, up to 9 nm.[132] The other acceptors applicable in TR-FRET with europium are Cy-5 [133,134] and its derivatives and to Alexa® dyes 647 [135] and –680.[136]

Europium emission is characterized by several transitions, (of which the magnetical dipole defined transition (${}^5\text{D}_0\text{--}{}^7\text{F}_1$) is not regarded as resonance partner) [137] Thus europium can potentially function as energy donor involving ${}^5\text{D}_0\text{--}{}^7\text{F}_2$ transition (613 nm), also the ${}^5\text{D}_0\text{--}{}^7\text{F}_4$ transition was found to be efficient donating transition. The NIR lines at 690–710 nm have been applied in TR-FRET for example using Alexa® 680 as acceptor in an assay of estradiol.[136]

Terbium(III) has also recently found applications in TR-FRET [138-141] and is commercialized by Invitrogen under the trade name Lanthascreen®. Terbium can donate energy to fluorescein through its first transition (${}^5\text{D}_4\text{--}{}^7\text{F}_6$), and can also transfer energy from the second transition (${}^5\text{D}_4\text{--}{}^7\text{F}_5$) to Cy-3, phycoerythrin, rhodamine derivatives or Alexa® dyes.

The dyad design can be modulated to give turn-“on” probes incorporating non-emitting acceptors (quenchers) such that cleavage increases signal (approach deemed Time-Resolved Fluorescence Quencher Assay - TR-FQA). TR-FQA has found applications in assays of hydrolyzing enzymes, such as proteases, where the flexibility of donor- and quencher-labeled substrate peptides, together with the long donor decay and efficient quenchers, allow highly efficient dynamic quenching and thus monitoring the enzymatic reaction.[142] Different substrate structures require somewhat different designs in respect to quenchers (overlap integral) and quenching efficiencies.[143,144] In protease multiplexing four luminescent lanthanides (europium, terbium, samarium, and dysprosium) have been tested and a triple-label assay was demonstrated for caspases 1, 3, and 6.[145]

An alternative electronic energy transfer mechanism to FRET is Dexter, and is particularly prevalent in inorganic multichromophore systems.[146] Triplet-triplet energy transfer via a Dexter mechanism is considered to be rather short range, see equation 4, where J is the integral overlap between the normalized donor emission and acceptor absorption spectra, L is the effective average Bohr radius of the excited and unexcited states of the donor and acceptor (0.7–6 Å, with an average value of 1.5 Å) [6], and K is the experimental factor.

$$k_{dexter} = KJ \exp\left(\frac{-2R_{DA}}{L}\right) \quad (\text{Eqn. 4})$$

For **18** (Figure 9), the alkane chain linker does not provide a good electronic interaction between energy donor (D) and energy acceptor (A), and the DA interaction is dipole–dipole in nature.[147] This energy transfer mechanism fits with a FRET treatment and the exoergonic Ru→Os energy transfer is moderately fast, k_{en} is $4.5 \times 10^8 \text{ s}^{-1}$ for **18**. In contrast, while for complex **19** the energetic and spatial (intermetal separation, d_{MM}) parameters are quite similar to those of **18**, the Ru→Os energy step is two orders of magnitude faster.[137] This results from the alkyne bridge providing an efficient electronic interaction between the D and A centres. As such a through-bond Dexter-type mechanism is involved. This phenomenon is shown to give rise to efficient transfer across surprisingly long distances, even as high as 42 Å in certain conjugated stems.[148]

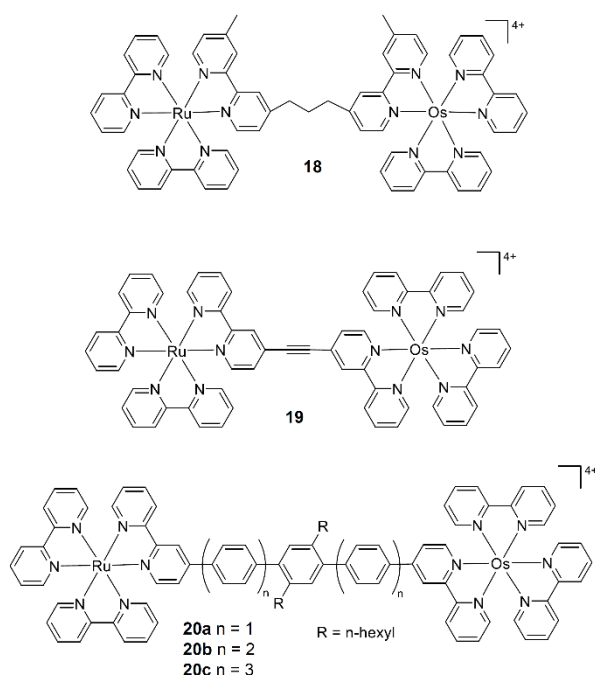


Figure 9. Examples of dyads comprising Ru(II)-donor and Os(II)-acceptors for EET studies.

Long distance energy transfer of excitation occurs in the series of complexes **20a** – **20c** in Figure 9. Here the modular approach is based on the inclusion within the bridge of a variable number

of spacer units, allowing the construction of dyads **20a**, **20b** and **20c**, where the photoactive units are separated by 3, 5 and 7 phenylene groups, respectively. The three dyads represent excellent models of rigid systems particularly suited for the study of Ru→Os energy over a distance of up to 42 Å. For these cases, it has been possible to conclude that the dipole–dipole mechanism cannot be responsible for the energy transfer step. Indeed, plotting $\ln(k_{en})$ against the intermetal separation, showed a linear dependence, consistent with the Dexter approach, equation 5.

(Eqn. 5)

$$k_{en} \propto \exp(-\beta d_{MM})$$

From these results an attenuation factor $\beta = 0.32 \text{ \AA}^{-1}$ has been evaluated, [149] while previous work dealing with the effect of polyphenylene spacers suggested $\beta = 0.66 \text{ \AA}^{-1}$. [150] It is noteworthy that nearly identical results are obtained at 77 K and at room temperature, [149, 150] showing that energy transfer, unlike electron transfer, is not affected by temperature or state of the fluid (or frozen) solvent. This is probably due to the reorganization energy, λ , for the energy transfer step being very close to the exothermicity, $-\Delta G$, of the process. [151]

Dexter transfer can be important to sensitize luminescence, for example in weakly absorbing lanthanide complexes, and its modulation by a target analyte can represent a signal transduction mechanism in chemosensors. Based on this premise, a prototype luminescent turn-on probe for Cu⁺ (and Ag⁺) was described (**21**, Figure 10), harnessing a selective binding site ($\log K_{ass} = 9.4$ and 7.3 for Cu⁺ and Ag⁺, respectively) based on the coordinating environment of the bacterial metallo-chaperone CusF, integrated with a terbium-ion-signaling moiety. [152] CusF is part of the CusCFBA system responsible for copper or silver detoxification in gram-negative bacteria. [153] CusF binds either Cu⁺ or Ag⁺ by the side chains of four amino acids: two methionines (M), a histidine (H), and a tryptophan (W) in Figure 10. [154,155]

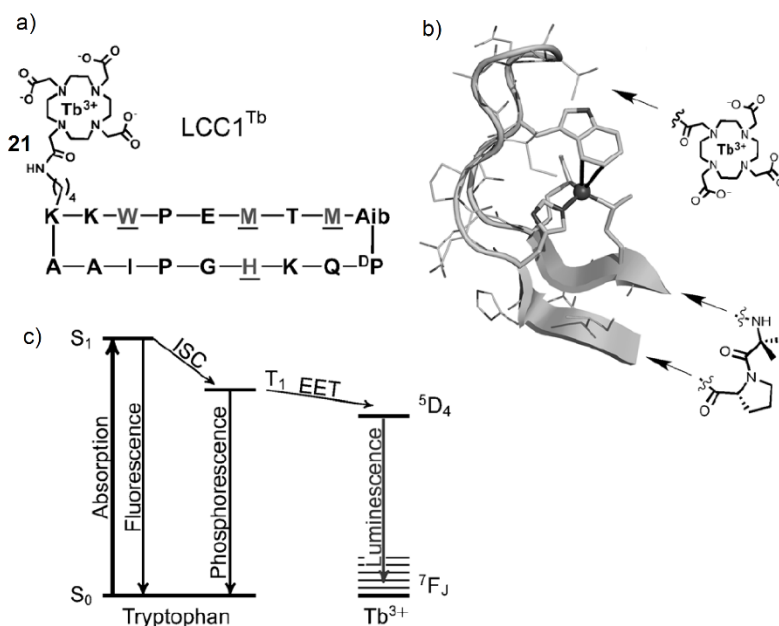


Figure 10. a) Amino acid sequence of LCC1Tb, chelating moieties are underlined; b) Principle of the probe design based on the X-ray structure of the Cu⁺ binding loop of CuSF; c) Simplified Jablonski–Perrin diagram of LCC1Tb probe and pertinent photophysical processes. Reproduced with permission from *Angew. Chem. Int. Ed.* **54**, 11453-11456 (2015).

Indeed while extracellular copper is in the +II oxidation state, mobile copper is in the reduced +I state in cells. The indole ring of the tryptophan establishes a cation–π interaction with the metal ion that red-shifts the π–π* transition of the indole and fully quenches its fluorescence. Metal cation–π interactions are known to efficiently enhance intersystem crossing (ISC) and increase the population of the excited triplet state of a fluorophore, thereby quenching the fluorescence.[156] The populated tryptophan triplet population, which subsequently sensitized (Figure 10c), on the microsecond timescale, the long-lived terbium emission, offering a novel approach in bioinspired chemosensor design.

An interesting example of Dexter-like energy transfer was recently reported between a nanomaterial, namely CdSe semiconductor quantum dots, and surface-bound polycyclic pyrene and anthracene hydrocarbon dyes pending green light photoexcitation of the former.[157] This demonstrator was of particular interest as it considered transfer between somewhat electronically different entities, i.e. from a quantum dot triplet exciton to a more well-defined formal organic molecular triplet state and opens the door to testing other nanomaterial-molecule interactions. In a previous study, involving similar entities, but where the core CdSe was covered with a ZnS protecting shell no such transfer was observed, the shell apparently acting as a barrier to transfer leading to orthogonal photophysical behaviour of the two components.[158] The population of surface bound organic triplets was evoked as sensitizers for chemical transformations, which equally may eventually take advantage of the large two photon cross-section of quantum dots for NIR excitation.

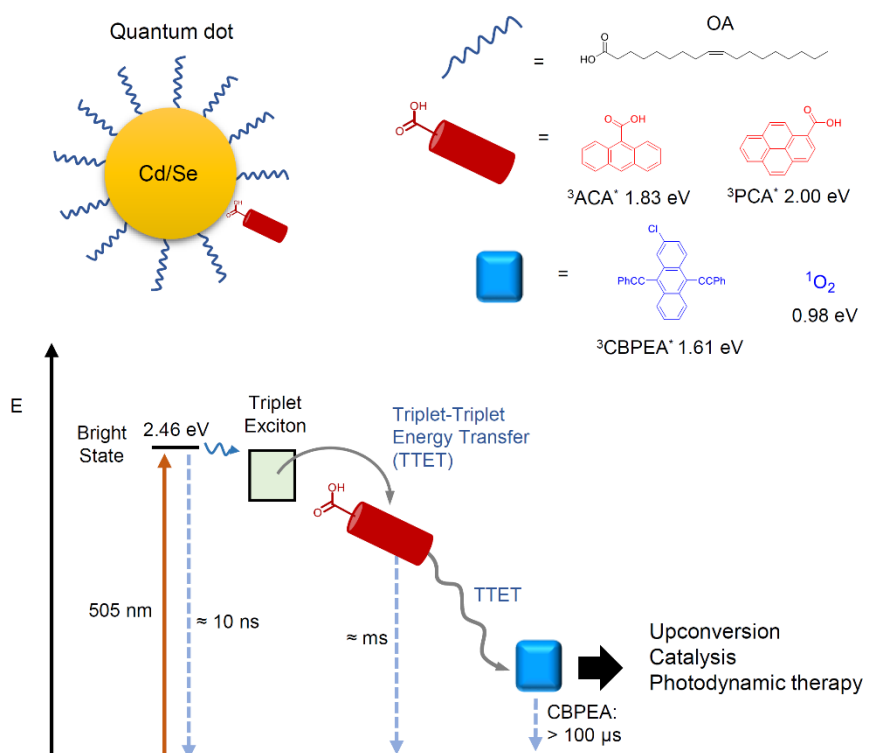


Figure 11. Inorganic semiconductor quantum dots as sensitizers of organic triplets and role in subsequent triplet transfer.

5.4.1 Reversible Electronic Energy Transfer

Electronic energy transfer considered above concerns primarily unidirectional processes, with energy being transferred from a higher energy to a lower-energy site/chromophore. An alternate scenario may exist in specific cases, whenever low-lying, relatively long-lived excited states on adjacent donor-acceptor chromophores are quasi-isoenergetic, when reversible intercomponent energy transfer can take place.[159-162] This Reversible Electronic Energy Transfer (REET) can greatly modify the observed properties of the supramolecular system compared to the individual components. More precisely, this can give rise to a prolonged luminescence lifetime, change the nature of the excited state and can be combined with other photophysical processes, such as photoinduced electron transfer. These properties are promising for applications as photosensitizers in multicomponent light-harvesting and sensor systems have been envisaged.

Due to the precise set of prerequisites, reversible electronic energy transfer (REET) has only been observed between triplet states in a rather small number of molecules, typically in transition

metal-organic chromophore conjugates, although this situation is changing. Importantly, bearing in mind the kinetic and energetic parameters detailed below are satisfied, a REET process can be engineered in a predetermined fashion in designer bichromophoric systems.[163-166]

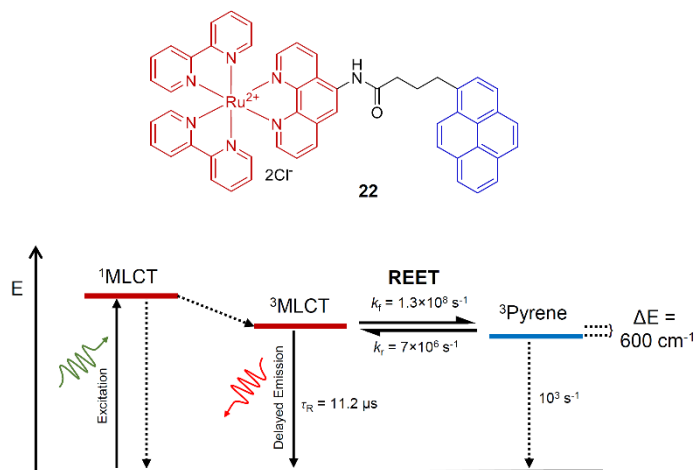


Figure 12. Structural formula of a prototype complex exhibiting intermolecular REET between a $\text{Ru}(\text{bpy})_3^{2+}$ and a pyrene chromophore, along with the corresponding Jablonski-Perrin diagram and rates of transfer and deexcitation.[159]

In terms of energy, the lowest-lying excited state energies of the partner chromophores must be close (i.e. $> 1000 \text{ cm}^{-1}$), such that available thermal energy is sufficient to overcome the energy gap between these lowest-lying excited states of each chromophore. Available energy is temperature dependent and at room temperature kT is a few kcal/mol. For example, in the prototype shown in Figure 12, the energy gap between matched chromophores (ΔE) is circa 600 cm^{-1} . [159] The distribution of energy between states in a population of excited molecules after thermal equilibration can be modelled based on a Boltzmann-type distribution taking ΔE and T into account.[167-169]

In order for REET to be efficient, forward and back energy transfer processes should be fast with respect to deexcitation, meaning that following excitation a dynamic equilibrium is established with respect to instantaneous energy localization. This equilibrium can be influenced by the presence of additional similar organic chromophores, which will increase the probability for energy to be located on the organic chromophore with respect to the metal centre. As energy is temporarily stored on the organic units before being ultimately emitted from the inorganic unit they are often described as energy reservoirs.

The ratio of populated organic triplets to $\text{Ru}(\text{bpy})_3^{2+}$ -like triplets excited molecules is denoted K_{eq} , which defines equilibrium. Studies of $\text{Ru}(\text{bpy})_3^{2+}$ -like chromophores bearing varying numbers of appended pyrene chromophores showed a linear increase in K_{eq} with the number of appended chromophores and the observed luminescence lifetime, τ . [170-171] On passing from 0 to 6 appended pyrenes, the lifetime

increased from 0.7 μs to 18.1 μs in degassed MeCN, where each chromophore added on average 2.7 μs . [170] The origin of the prolonged luminescence lifetime with respect to the parent chromophore can be rationalized according to equation 6. Here τ_{obs} is the measured luminescence lifetime, τ_0 is the luminescence lifetime of the emissive parent chromophore, α is the proportion of excited $\text{Ru}(\text{bpy})_3^{2+}$ -like triplets, and $1-\alpha$ is the proportion of pyrene-like triplets. The resulting lifetime is a weighted average of the contribution of each chromophore, in terms of the inherent lifetime and population.

(Eqn. 6)

$$\frac{1}{\tau_{obs}} = \alpha \frac{1}{\tau_{obs}} + (1 - \alpha) \frac{1}{\tau_{pyr}}$$

In the supramolecular ensemble the contribution of the more persistent organic triplet states, which have inherent lifetimes circa two orders of magnitude higher than typical $^3\text{MLCT}$ states is decisive. This difference in deexcitation rate further ensures that energy will be primarily emitted from the inorganic moiety. When energy transfer processes are efficient, observed quantum yields have proved to be essentially unaffected with respect to the parent luminophore. The initial approach to equilibrium following excitation, corresponds to a sum of the rate constants for forward (k_f) and backward (k_b) energy transfer and a short-lived emission component (typically ps to ns) in addition to the long-lived luminescence emanating from the equilibrated excited states corresponds to this process.

Development of REET systems has evolved from covalently-tethered dyads towards non-covalent assemblies, and a few representative examples, illustrated in Figure 13, will be considered below. For a more comprehensive analysis the reader is referred to some recent reviews. [163-166]

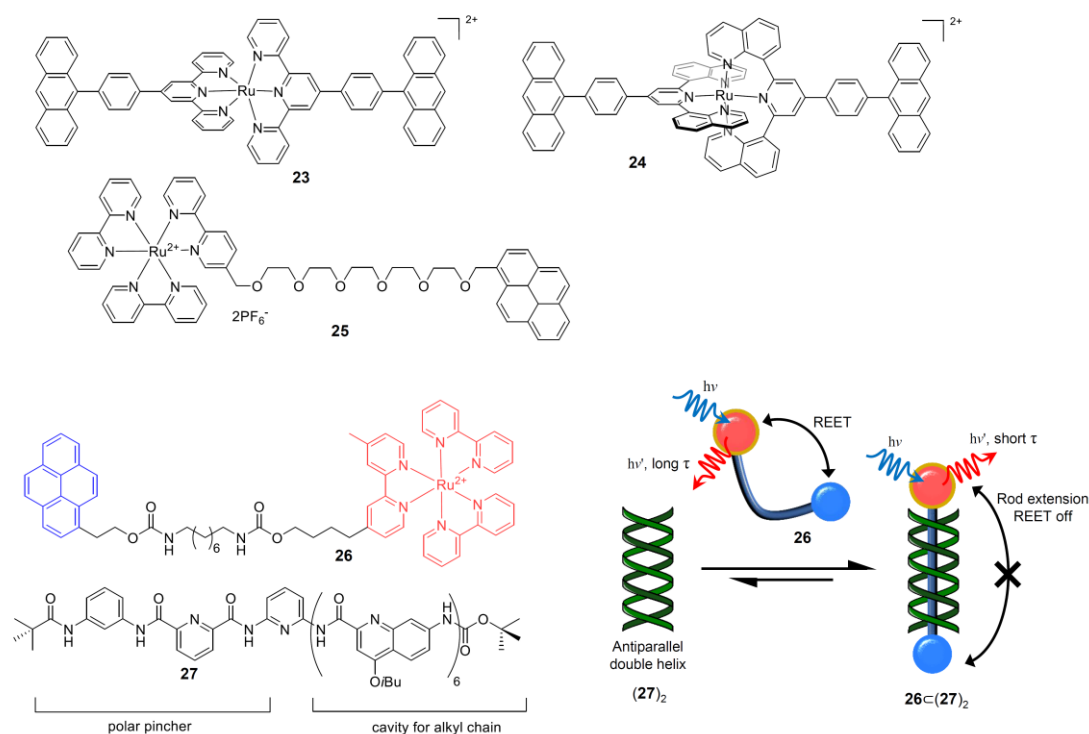


Figure 13. Bichromophoric hybrid organic-inorganic dyads exhibiting reversible interchromophore EET (REET).

Ruthenium (II) bis(terpyridine) complexes are an important class of compound, offering access to structures including linear geometries.[172] However, their luminescence properties are typically inhibited by thermally-accessible metal-centred states. [Ru(tpy)₂]²⁺ (tpy = 2,2';6',2''-terpyridine) has a correspondingly low emission quantum yield (<10⁻⁵) and short lifetime (0.25 ns).[173] The photophysical properties may be improved by design, on defavouring thermally-activated loss by increasing the energy gap between states on lowering emissive ³MLCT levels, as a result of incorporating highly electron poor tpy-like ligands.[174] Furthermore, integration of a complementary anthracene chromophore led to luminescence lifetimes as long as 1.8 μs (**23**, Figure 13) but with a similarly low quantum yield.[175] More recently, ruthenium complexes exhibiting microsecond luminescence lifetimes were reported on replacing the two external pyridine moieties of tpy with quinolines in constituent ligands, which offers an optimized octahedral coordination environment.[176] Grafting peripheral matched chromophores yielded **24**, a tridentate ruthenium complex with an unprecedented luminescence lifetime (τ_{em} = 42 μs) as a result of REET. Time-resolved spectroscopies showed that excited-state equilibration is reached in less than 400 picoseconds with an average of 94% of energy being stocked on the organic energy reservoir in the equilibrated system prior to delayed MLCT emission.[177] While the focus above was on ruthenium (II) complexes the kinetic scheme is similarly valid for other bichromophore systems based on metals including Ir, Re, Pt, Os W.[166]

Concerning non-covalent assemblies, a recent foldamer on an axel structure (deemed a foldaxane) was reported exhibiting REET.[178] Molecular thread **26** is flexible in solution, allowing the free approach of the two chromophores while in the excited-state excited and REET to occur, giving the anticipated delayed luminescence seen previously with **25**. [179] Meanwhile foldamer (**27**), dimerizes in solution giving double stranded helicate (**27**)₂ with a void that can accommodate linear molecules and bind them with two hydrogen bonds. Mixing (**27**)₂ and **26** causes formation of the host:guest complex as the thread penetrates the double helix distancing the chromophores and blocking the REET. Based on resulting lifetime changes, real-time threading can be observed. The foldaxane assembly thus is a demonstrator for the potential of REET in lifetime-based conformation probes.

With REET giving rise to long lived luminescence, application as photosensitizers for diffusion-limited processes may be considered. Recently, this property was harnessed in a sensitized triplet–triplet annihilation (TTA) of anthracene triplets in aqueous solution.[180] TTA represents one manifestation of solar energy conversion.[181] Thus green-to-violet upconversion with unprecedented quantum yields in pure water, which was further used to drive a dehalogenation reaction, proposed for photochemical water cleaning. To further illustrate the scope of REET, this process was recently demonstrated between quantum dots and organic dyes. [182,183]

Thermally activated delayed fluorescence (TADF) is a process reminiscent of REET (with the notable exception that the emitter is of singlet character), and has been championed as a means to greatly improve the output in OLED devices by harvesting triplets generated from electron-hole recombination.[184] While successful TADF functional materials are generally organic, copper complexes such as **28** (Figure 14) have recently been proposed.[185] Indeed, the close proximity of singlet and triplet states has been a matter of discussion from several years.[186] Complex **28** is a strongly luminescent neutral copper(I) complex exhibiting very strong blue/white luminescence with emission quantum yields of up to 90%. Below 100 K, the triplet MLCT emission decay times are in the order of many hundreds of microseconds. On increasing the temperature, the emission decay time is drastically reduced to 13 ns at ambient temperature and emit strongly as neat material or doped into poly(methyl methacrylate) (PMMA).

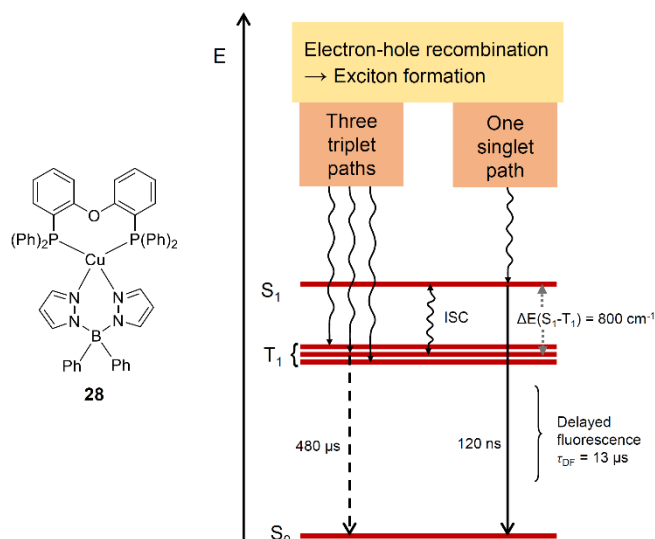


Figure 14. Reversible ISC giving rise to delayed fluorescence, representing an approach to improve OLED efficiency.

This is assigned to delayed fluorescence from an efficient thermal population of a ¹MLCT, which lies only 800 to 1300 cm⁻¹ above the triplet state, depending on the individual complex. For applications in OLEDs and LEECs, for example, this type of thermally activated delayed fluorescence (TADF) creates a new mechanism that allows to harvest both singlet and triplet excitons (excitations) in the lowest singlet state. This effect of singlet harvesting leads to drastically higher radiative rates than obtainable for emissions from triplet states of Cu(I) complexes.

5.4.2 Photoinduced Electron Transfer

Electron transfer is possibly the most important reaction on earth. It plays a key role in photosynthesis as discussed in previous sections and also in charge separation / photovoltaic devices. As such, it has been a focus of study for several decades. In this section, space precludes an exhaustive treatment of this subject, and interested readers are referred to some leading reviews and reference works on the topic, including inorganic complexes interfacing biological systems.[187-191] Rather, a brief overview of some topics of recent interest will be given and implementation in photoactive supramolecular architectures designed in the goal of applications in sensing and information storage will be presented.

Photoinduced Electron Transfer (PET) between components in a tethered system is represented in Figure 15a, which is equally applicable to a non-covalent assembly. Upon photoexcitation an

electron may be transferred rapidly (during the lifetime of the excited state) from D (donor) to A (acceptor) across the bridge (B). Ultimately a fast back electron transfer may occur. In some cases this may be beneficial (to reset a system and avoid radical reactions) or less so, if long lived charge separation is required. Formation of the transient species (*D-B-A, D⁺-B-A⁻, D-B-*A) and kinetics can be followed by transient absorption (UV-vis-NIR) on different timescales along with time-resolved fluorescence experiments. Figure 15b shows some prototype designer D-B-A systems, where B is saturated and rigid, and D and A are attached with no orientational freedom.[192-195] For an example of rigid inorganic scaffolds see Figure 9 and examples in references, which were designed with the goal of prolonged charge separation. [196-198]

Investigated systems shown in Figure 15b span a range of centre-to-centre D-A distances of 7-15 Å and of 4 to 12 interposed C-C bonds. For a linear arrangement of the connector B the rate constants decrease exponentially with distance. According to equation 7, k_{ET} corresponds to the rate of electron transfer quenching, r is distance between donor and acceptor, β is the attenuation factor dependent on properties of the medium separating fluorophore and quencher.

$$k_{ET} \propto e^{-\beta r} \quad (\text{Eqn. 7})$$

Electron transfer takes place via a through-bond coupling and are consistent with theoretical predictions that an all-trans arrangement of π bonds are optimal for through bond interactions.[199,200]

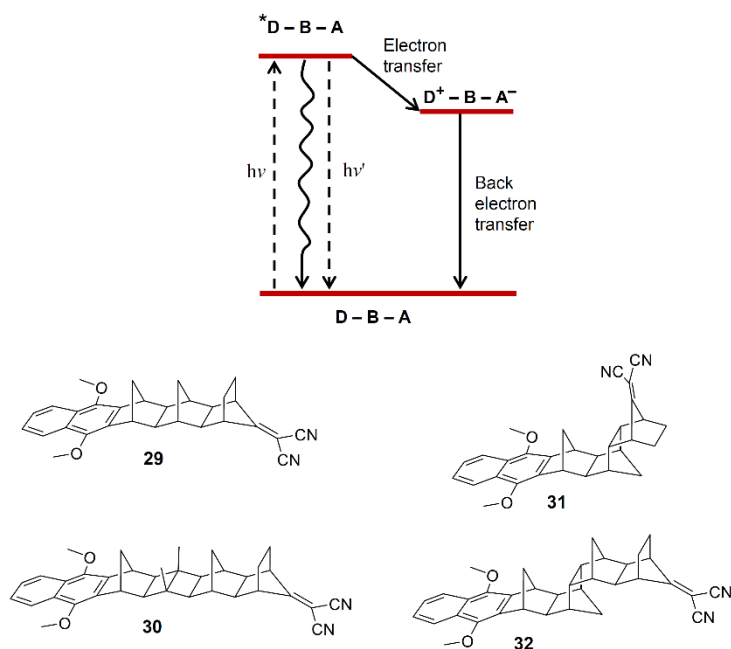


Figure 15. Schematic representation of photoinduced electron transfer processes in a supramolecular system made of donor (D) and acceptor (A) components linked by a connector (B). Dimethoxynaphthalene-dicyanovinyl dyads with rigid bridges.[194,195]

The driving force for photoinduced electron transfer (ΔG^0) can be estimated in multicomponent supramolecular systems as represented in Equation 8, using the simplified Rehm-Weller equation.[201]

$$\Delta G^0 = E_{D^+/D}^0 - E_{A/A^-}^0 - \Delta H_{solv} - \frac{e^2}{4\pi\epsilon r} \quad (\text{Eqn. 8})$$

$E_{D^+/D}^0$ is the donor oxidation potential, E_{A/A^-}^0 is the acceptor reduction potential, e is the electron charge, ϵ is the solvent dielectric constant and r is the distance between the two ions. Additionally, in solution two further terms consider the solvation effect (ΔH_{solv}) and the Coulombic energy ($\frac{e^2}{4\pi\epsilon r}$) of the formed radical ion pair. Importantly, based on redox properties and excited state energies of constituent components the driving force can be calculated in advance when there is weak coupling.

PET has been successfully used in photoluminescent molecular chemosensors.[22-24] Indeed with favourable energetics, if distances are sufficiently short, electron transfer can kinetically compete with luminescence. To design a turn-on PET sensor, several modules are required: the primary units are a luminescent reporter and a redox-active receptor. The later provides the selectivity of the sensor to a given analyte and largely to the sensitivity. The receptor and emitter should be sufficiently close to ensure that once the chromophore is excited, a favourable receptor to chromophore quenching ET process takes place, switching “off” the luminescence. On the other hand, when an analyte binds at the receptor and electron transfer is disfavoured, luminescence would be switched “on”. Of course there are other variants of this general scheme, for example quenching may occur by oxidative rather than reductive quenching. Introduction of a short saturated spacer, such as a methylene group, between receptor and emitter may judiciously be introduced in order to minimize the mutual interactions of the constituent components, whilst assuring an efficient PET process.[22] Figure 16a shows a representation of frontier molecular orbitals and how they are modified by guest binding. **33** comprises a luminescent Re(I) polypyridyl unit coupled to an azacrown ether-type receptor for metal ion guests.[202] In the absence of Ca^{2+} a relatively low luminescence quantum yield and shortened excited-state lifetime of **33** is observed, which may be attributed to a PET process from the aniline-like donor to the luminophore (Figure 16b). Calcium ion binding in **34** leads to an 8-fold enhancement, as quenching pathways are disfavoured. (An alternative/complementary explanation can be due to a non-emissive arylazacrown to bipyridine ligand-to-ligand charge transfer (LLCT) state evolving into the emissive MLCT state).

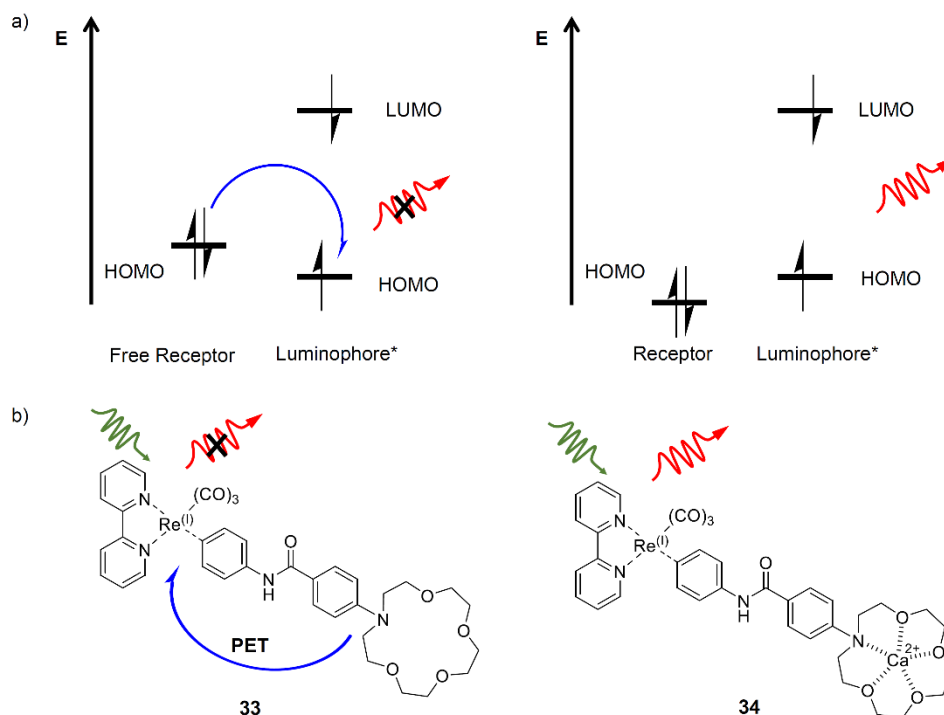


Figure 16. a) PET from a donor to an excited luminophore quenching luminescence, abated on binding (or reacting with) an analyte; b) A Ca²⁺-sensing luminescent Re(I) polypyridine complex.

Metal-to-Metal Electron Transfer is regarded as a means to design switchable coordination compounds.[203,204] Since the first reports of photomagnetic effects in Prussian blue Fe/Co networks, a substantial chimiotheque of molecular analogues have been developed, allowing studies of metal-to-metal electron transfer by investigating their structural, spectroscopic, electrochemical and magnetic properties. In these molecules, the presence of electronic donor and acceptor moieties promotes a reversible transfer of one electron between the two sites through temperature change and/or low temperature photoexcitation. The modification of the optical and magnetic states by light irradiation allows magneto-optical bistability. Different donor/acceptor couples have been considered in molecular compounds, such as radicals or complexes, implying an electron transfer (ET) between an organic moiety (radical/ligand) and a metal centre or between two metal ions.[205,206] In this later case, Fe/Co Prussian blue analogues (PBAs) have emerged as one of the most interesting systems, due to their outstanding photoswitchable physical properties. These cyanido-bridged bimetallic tridimensional coordination networks, with general formula A_xCo_y[Fe(CN)₆]_nH₂O (A: alkaline ion), can display both optical and magnetic bistability due to a reversible metal-to-metal electron transfer process between the cobalt and iron centres, switching between paramagnetic (FeIII LS–CN–CoII HS) and diamagnetic (FeII LS–CN–CoIII LS) configurations- (Figure 17a; with LS: Low Spin and HS: High Spin). This phenomenon has been named as charge-transfer-induced spin transition (CTIST).[207] Recently, numerous research groups have been involved in the transfer of these electronic properties to new Fe/Co coordination networks of lower dimensionality (2D, 1D or

OD) has emerged as an attractive research goal to develop new materials that can be easily manipulated and integrated into devices.

Figure 17b shows an example of a molecular square, a tetranuclear $[\text{Fe}_2\text{Co}_2]$ complex $\{[(\text{Tp}^*)\text{FeIII}(\text{CN})_3]_2[\text{CoII}(\text{bpy})_2]_2\}[\text{OTf}]_{24}\text{DMF}\cdot 2\text{H}_2\text{O}$ (**35**, Tp^* : tris(3,5 dimethyl)pyrazolyl borate, OTf : trifluoromethanesulfonate), exhibiting thermally reversible and light-induced electron transfer.[208] ET phenomena were studied by magnetic measurements (Figure 17, bottom). At high temperature, the χT value of $6.8 \text{ cm}^3 \text{ K mol}^{-1}$ agreed well with the presence of two FeIII LS and two CoII HS magnetic centres. By decreasing the temperature, an abrupt decay of the χT product was observed around 168 K reaching $0.4 \text{ cm}^3 \text{ K mol}^{-1}$ at 120 K. This result confirmed the expected thermal electron transfer between CoII HS and FeIII LS leading to the conversion of paramagnetic $[\text{FeIII} \text{LS} \text{CoII} \text{HS}]$ pairs into diamagnetic $[\text{FeII} \text{LS} \text{CoIII} \text{LS}]$ ones. The photomagnetic properties were studied at 10 K by irradiation of the sample with white light. A sharp increase of the χT product was observed in agreement with the photogeneration of paramagnetic FeIII LS– CoII HS pairs.

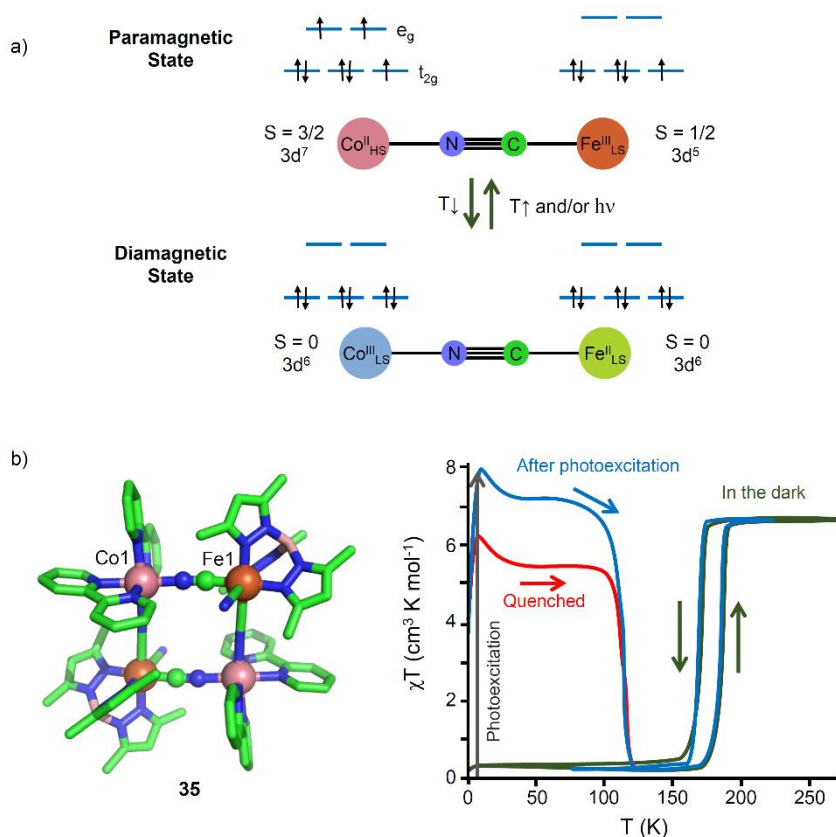


Figure 17. a) Schematic representation of switching between low spin (LS) and high spin (HS) states in a Co/Fe system; b) A molecular square showing photoswitched magnetism at low T.

Photoinduced metastable states were found to relax with relatively long characteristic times, this $[\text{Fe}_2\text{Co}_2]$ molecular square possesses a relaxation time estimated at 3 minutes at 120 K. For discussion on Intra Valence Charge Transfer complexes, see reference [209].

5.5 Other photoactive multicomponent systems and approaches

In this chapter and other chapters in this section, a wide range of different examples and aspects in the growing area of inorganic supramolecular photochemistry were presented. In this short section a few remaining topics will be cited that are either thematically peripheral or less well-represented in the literature.

Surface functionalized metal nanoparticles and semiconductor quantum dots represents a vast body of work. As is their deposition into ordered layers for photonic applications. While a few examples of luminescent quantum dots are cited above, this is largely out of the scope of this chapter. For a review on luminescent quantum dot-molecular conjugates, see [210].

Supramolecular transfer of chirality from enantiopure ligands to metal ions gives “chiral at metal” complexes and assemblies. Such chiral complexes are of interest in materials science for chiral switches and molecular machines, biological mimics, and Circularly Polarized Luminescence (CPL) probes.[211,212] Such a chiroptical signature and can be used as probes of chemical and biological environments. Among this class of compounds, helicates hold a privileged position, and can be produced using many multidentate ligands and metal centers and may be considered as artificial mimics of protein helices, promising biologically active substances, and attractive molecules in materials science. The chirality in polyoxometalates is another growing field because many applications are foreseen in asymmetric catalysis, magnetism, medicine, sensing.

5.6 Conclusion

In recent years supramolecular photochemistry has greatly advanced, driven by chemists' imagination and inspired by nature. The development of laser technologies and microscopes has further aided studies with high spatial and temporal resolution.

While organic systems have no doubt been more studied in general, inorganic variants and hybrid organic: inorganic molecules and nanostructures structures are greatly emerging, taking advantage of reversible redox properties of metals and distinct coordination geometries, to generate specific functional molecular architectures and nanostructured materials. Equally,

long-lived luminescence, circularly polarized luminescence and red and NIR emission are desirable luminescence properties along with high photostability.

A diversity of supramolecular interactions (including hydrogen-bonding, hydrophobic interactions, π -stacking) as well as metal-specific interactions are available in Nature's toolbox to develop non-covalent assemblies, smart materials and potentially interface biological systems. Such supramolecular systems are laying out design principles for artificial photosynthesis and fundamental studies of electron transfer, proton coupled electron transfer and electronic energy transfer.

Future progress in the area of supramolecular inorganic photochemistry will no doubt equally consider out of equilibrium dynamic systems, chiral luminescent materials and self-assembling and self-healing molecular electronics.

Acknowledgements

V. M-C. thanks the European Union for the MSCA-IF. This project has received funding from the European Union's Horizon 2020 research and innovation programme under the Marie Skłodowska-Curie grant agreement No 796612. N. McC. thanks the CNRS for support.

List of abbreviations

AFM: Atomic Force Microscopy

AIE: Aggregate-Induced Emission

ATP: Adenosine Triphosphate

Bpy: 2,2'-Bipyridine

CD: Circular Dichroism

CusF: Cation efflux system protein

CusCFBA: Copper-Transporting Efflux System

DAC: Diamond Anvil Cell

DFT: Density Functional Theory

EET: Electronic energy transfer

ET: Electron Transfer

FRET: Förster Resonance Energy Transfer

H: Histidine (amino acid)

HOMO: Highest Occupied Molecular Orbital

HS: High Spin

ICT: Internal Charge Transfer

ILCT: Interligand Charge Transfer

ISC: Intersystem Crossing

LC: Ligand Centred

LEECs: Light Emitting Electrochemical Cells

LLCT: Ligand-To-Ligand Charge Transfer

LMCT: Ligand to Metal Charge Transfer

LS: Low Spin

LUMO: Lowest Unoccupied Molecular Orbital

M: Methionine

MC: Metal Centred

MLCT: Metal-to-Ligand Charge Transfer

MMCT: Metal-to-Metal Charge Transfer

MMLCT: Metal-Metal-To-Ligand Charge Transfer

MO: Molecular Orbital

NADP⁺: Nicotinamide Adenine Dinucleotide Phosphate

NADPH: Reduced form of NADP⁺

NIR: Near Infrared

OLED: Organic Light-Emitting Diode

OTf: Trifluoromethanesulfonate

PET: Photoinduced Electron Transfer

PCT: Photoinduced Charge Transfer

Phen: 1,10-Phenanthroline

PMMA: Poly(methyl methacrylate)

REET: Reversible Electronic Energy Transfer

RNS: Reactive Nitrogen Species

ROS: Reactive Oxygen Species

TADF: Thermally Activated Delayed Fluorescence

Terpy or tpy: 2,2':6',2''-Terpyridine

TFA: Trifluoroacetic Acid

Tp*: Tris(3,5 dimethyl)pyrazolyl borate

TTA: Triplet–Triplet Annihilation

TRF: Time-Resolved Fluorometry

TR-FQA: Time-Resolved Fluorescence Quenching Assay

TR-FRET: Time-Resolved Förster Resonance Energy Transfer

W: Tryptophan (aminoacid)

ΔE : Energy Gap

References

1. J.-M. Lehn, *Supramolecular Chemistry: Concepts and Perspectives*, Wiley-VCH, Weinheim (1995).
2. C. A. Hunter, *Angew. Chem. Int. Ed.* **43**, 5310–5324 (2004).
3. V. Balzani and F. Scandola, *Supramolecular Photochemistry*; Horwood: Chichester, U.K. (1991).
4. V. Balzani, *Tetrahedron* **48**, 10443–10514 (1992).
5. D. A. Uhlenheuer, K. Petkau and L. Brunsveld, *Chem. Soc. Rev.* **39**, 2817–2826 (2010).
6. L. L. Kiessling and A. C. Lamanna, Multivalency in Biological Systems. In: Schneider M.P. (eds) *Chemical Probes in Biology*. NATO Science Series (Series II: Mathematics, Physics and Chemistry), vol 129, pp 345–357. Springer, Dordrecht (2003).
7. D. Philp and J. F. Stoddart, *Angew. Chem., Int. Ed. Engl.* **35**, 1154–1196 (1996).
8. D. Natale and J. C. Mareque-Rivas, *Chem. Commun.* 425–437 (2008).
9. S. Rau, B. Schäfer, S. Schebesta, A. Grüßing, W. Poppitz, D. Walther, M. Duati, W. R. Browne and J. G. Vos, *Eur. J. Inorg. Chem.* 1503–1513 (2003).
10. P. J. F. de Rege, S. A. Williams and M. J. Therien, *Science* **269**, 1409–1413 (1995).

11. C. M. White, M. F. Gonzalez, D. A. Bardwell, L. H. Rees, J. C. Jeffery, M. D. Ward, N. Armaroli, G. Calogero and F. Barigelletti, *J. Chem. Soc., Dalton Trans.* 727–736 (1997).
12. J.-P. Sauvage, J.-P. Collin, J.-C. Chambron, S. Guillerez, C. Coudret, V. Balzani, F. Barigelletti, L. De Cola and L. Flamigni, *Chem. Rev.* **94**, 993–1019 (1994).
13. V. Balzani, A. Juris, M. Venturi, S. Campagna and S. Serroni, *Chem. Rev.* **96**, 759–833 (1996).
14. Proton Transfer in Hydrogen Bonded Systems, ed. T. Bountis, Plenum, New York (1992).
15. P. M. Krasilnikov, P. A. Mamonov, P. P. Knox, V. Z. Paschenko and A. B. Rubin, *Biochim. Biophys. Acta* 1767, 541–549 (2007).
16. J. M. Mayer, *Annu. Rev. Phys. Chem.*, **55**, 363–390 (2004).
17. J. A. Roberts, J. P. Kirby and D. G. Nocera, *J. Am. Chem. Soc.* **117**, 8051–8052 (1995).
18. C. Turro, C. K. Chang, G. E. Leroi, R. I. Cukier and D. G. Nocera, *J. Am. Chem. Soc.*, **114**, 4013–4015 (1992).
19. J. P. Kirby, N. A. van Dantzig, C. K. Chang and D. G. Nocera, *Tetrahedron Lett.* **36**, 3477–3480 (1995).
20. R. I. Cukier, *J. Phys. Chem.* **98**, 2377–2381 (1994).
21. R. I. Cukier, *J. Phys. Chem.* **100**, 15428–15443 (1996), and refs. therein.
22. A. P. de Silva, H. Q. N. Gunaratne, T. Gunnlaugsson, A. J. M. Huxley, C. P. McCoy, J.T. Rademacher and T.E. Rice, *Chem. Rev.* **97**, 1515–1566 (1997).
23. B. Valeur and I. Leray, *Coord. Chem. Rev.* **205**, 3–40 (2000).
24. X. H. Li, X. H. Gao, W. Shi and H. M. Ma, *Chem. Rev.* **114**, 590–659 (2014).
25. T. Gunnlaugsson, M. Glynn, G. M. Tocci, (née Hussey), P.E. Kruger and F. M. Pfeffer, *Coord. Chem. Rev.* **250**, 23–24, 3094–3117 (2006).
26. E. M. Nolan and S. J. Lippard, *Chem. Rev.* **108**, 3443–3480 (2008).
27. P. A. Gale and C. Caltagirone, *Coord. Chem. Rev.* **354** 2–27 (2018).
28. P. D. Beer, F. Szemes, V. Balzani, C. M. Salá, M. G. B. Drew, S. W. Dent and M. Maestri, *J. Am. Chem. Soc.* **119**, 11864–11875 (1997).
29. S. Sun and A. J. Lees, *Chem. Commun.* 1687–1688 (2000).
30. A. Chatterjee, M. Santra, N. Won, S. Kim, J. K. Kim and S. Kim, *J. Am. Chem. Soc.* **131**, 2040–2041 (2009).
31. Y. Hitomi, T. Takeyasu, T. Funabiki and M. Kodera, *Anal. Chem.* **83**, 9213–9216 (2011).
32. G. M. Whitesides, J. P. Mathias and C T. Seto, *Science* **254**, 1312–1319 (1991).

33. T. Aida, E. W. Meijer and S. I. Stupp, *Science* **335**, 813–817 (2012).
34. J.-M. Lehn, *Proc. Natl Acad. Sci. USA* **99**, 4763–4768 (2002).
35. J.-M. Lehn, *Angew. Chem. Int. Ed. Eng.* **29**, 1304–1319 (1990).
36. M. Mauro, A. Aliprandi, D. Septiadi, N. Seda Kehra and L. De Cola, *Chem. Soc. Rev.* **43**, 4144–4166 (2014).
37. J. Muñiz, C. Wang and P. Pyykkö, *Chem.–Eur. J.* **17**, 368–377 (2011).
38. V. H. Houlding and V. M. Miskowski, *Coord. Chem. Rev.* **111**, 145–152 (1991).
39. V. M. Miskowski and V. H. Houlding, *Inorg. Chem.* **30**, 4446–4452 (1991).
40. C. A. Strassert, M. Mauro and L. De Cola, *Adv. Inorg. Chem.* **63**, 48–103 (2011).
41. I. M. Sluch, A. J. Miranda, O. Elbjeirami, M. A. Omary and L. M. Slaughter, *Inorg. Chem.* **51**, 10728–10746 (2012).
42. B. Ma, J. Li, P. I. Djurovich, M. Yousufuddin, R. Bau and M. E. Thompson, *J. Am. Chem. Soc.* **127**, 28–29 (2005).
43. D. Kim and J. L. Brédas, *J. Am. Chem. Soc.* **131**, 11371–11380 (2009).
44. M. Kato, C. Kosuge, K. Morii, J. S. Ahn, H. Kitagawa, T. Mitani, M. Matsushita, T. Kato, S. Yano and M. Kimura, *Inorg. Chem.*, **38**, 1638–1641 (1999).
45. H. B. Gray and A. W. Maverick, *Science* **214**, 1201–1205 (1981).
46. G. Gliemann and H. Yersin, *Struct. Bonding* **62**, 89–150 (1985) and references therein.
47. S. Y.-L. Leung, W. H. Lam and V. W.-W. Yam, *Proc. Natl. Acad. Sci. USA.* **11**, 7986–7991 (2013).
48. V. W.-W. Yam, K. M.-C. Wong and N. Zhu, *J. Am. Chem. Soc.* **124**, 6506–6507 (2002).
49. X. Zhang, B. Cao, E. J. Valente and T. K. Hollis, *Organometallics* **32**, 752–761 (2013).
50. Y. Tanaka, K. M.-C. Wong and V. W.-W. Yam, *Chem. Sci.* **3**, 1185–1191 (2012).
51. L.-Y. Zhang, L.-J. Xu, X. Zhang, J.-Y. Wang, J. Li and Z. N. Chen, *Inorg. Chem.* **52**, 5167–5175 (2013).
52. Y. Sun, K. Ye, H. Zhang, J. Zhang, L. Zhao, B. Li, G. Yang, B. Yang, Y. Wang, S.-W. Lai and C.-M. Che, *Angew. Chem. Int. Ed.* **118**, 5738–5741 (2006).
53. W. Zhang, W. Jin, T. Fukushima, N. Ishii and T. Aida, *Angew. Chem., Int. Ed.* **48**, 4747–4750 (2009).
54. V. N. Kozhevnikov, B. Donnio and D. W. Bruce, *Angew. Chem., Int. Ed.*, **47**, 6286–6289 (2008).

55. Y. Li, E. S.-H. Lam, A. Y.-Y. Tam, K. M.-C. Wong, W. H. Lam, L. Wu and V. W.-W. Yam, *Chem.–Eur. J.* **19**, 9987–9994 (2013).
56. N. K. Allampally, C. A. Strassert and L. De Cola, *Dalton Trans.* **41**, 13132–13137 (2012).
57. A. Y.-Y. Tam and V. W.-W. Yam, *Chem. Soc. Rev.* **42**, 1540–1567 (2013).
58. T. Cardolaccia, Y. Li and K. S. Schanze, *J. Am. Chem. Soc.* **130**, 2535–2545 (2008).
59. L. J. Chen, J. Zhang, J. He, X. D. Xu, N. W. Wu, D. X. Wang, Z. Abliz and H. B. Yang, *Organometallics* **30**, 5590–5594 (2011).
60. J. Zhang, X. D. Xu, L. J. Chen, Q. Luo, N. W. Wu, D. X. Wang, X. L. Zhao and H. B. Yang, *Organometallics* **30**, 4032–4038 (2011).
61. C. A. Strassert, C.-H. Chien, M. D. Galvez Lopez, D. Kourkoulos, D. Hertel, K. Meerholz and L. De Cola, *Angew. Chem., Int. Ed.* **50**, 946–950 (2011).
62. S. Y.-L. Leung and V. W.-W. Yam, *Chem. Sci.* **4**, 4228–4234 (2013).
63. M.-Y. Yuen, V. A. L. Roy, W. Lu, S. C. F. Kui, G. S. M. Tong, M.-H. So, S. S.-Y. Chui, M. Muccini, J. Q. Ning, S. J. Xu and C.-M. Che, *Angew. Chem., Int. Ed.* **47**, 9895–9899 (2008).
64. M. C.-L. Yeung and V. W.-W. Yam, *Chem. Sci.* **4**, 2928–2935 (2013).
65. V. W.-W. Yam, K. H.-Y. Chan, K. M.-C. Wong and N. Zhu, *Chem.–Eur. J.* **11**, 4535–4543 (2005).
66. C.-M. Che, C.-F. Chow, M.-Y. Yuen, V. A. L. Roy, W. Lu, Y. Chen, S. S.-Y. Chui and N. Zhu, *Chem. Sci.* **2**, 216–222 (2011).
67. C. Yu, K. H.-Y. Chan, K. M.-C. Wong and V. W.-W. Yam, *Proc. Natl. Acad. Sci USA* **103**, 19652–19657 (2006).
68. C. Yu, K. H.-Y. Chan, K. M.-C. Wong and V. W.-W. Yam, *Chem.–Eur. J.* **14**, 4577–4584 (2008).
69. K. M.-C. Wong and V. W.-W. Yam, *Acc. Chem. Res.* **44**, 424–434 (2011).
70. M. Mauro, A. Aliprandi, C. Cebrián, D. Wang, C. Kübel and L. De Cola, *Chem. Commun.* **50**, 7269–7272 (2014).
71. A. Aliprandi, M. Mauro and L. De Cola, *Nat. Chem.* **8**, 10–15 (2015).
72. E. Chardon, G. Dahm, G. Guichard and S. Bellemin-Laponnaz, *Organometallics* **31**, 7618–7621 (2012).
73. T. C. Johnstone, J. J. Wilson and S. J. Lippard, *Inorg. Chem.* **52**, 12234–12249 (2013).
74. F. Arnesano, M. Losacco and G. Natile, *Eur. J. Inorg. Chem.* 2701–2711 (2013).
75. V. Vreshch, W. Shen, B. Nohra, S. K. Yip, V. W.-W. Yam, C. Lescop and R. Réau, *Chem.–Eur. J.* **18**, 466–477 (2012) and references therein.

76. V. W.-W. Yam and E. C.-C. Cheng, *Chem. Soc. Rev.* **37**, 1806–1813 (2008).
77. V. W.-W. Yam and K. K.-W. Lo, *Chem. Soc. Rev.* **28**, 323–334 (1999).
78. L. H. Doerrer, *Dalton Trans.* **39**, 3543–3553 (2010).
79. J. Lefebvre, R. J. Batchelor and D. B. Leznoff, *J. Am. Chem. Soc.* **126**, 16117–16125 (2004).
80. U. Patel, H. B. Singh and G. Wolmershuäser, *Angew. Chem., Int. Ed.* **44**, 1715–1717 (2005).
81. A. J. Goshe, I. M. Steele and B. Bosnich, *J. Am. Chem. Soc.* **125**, 444–451 (2003).
82. M. J. Mayoral, C. Rest, V. Stepanenko, J. Schellheimer, R. Q. Albuquerque and G. Fernandez, *J. Am. Chem. Soc.* **135**, 2148–2151 (2013).
83. J. C. Lima and L. Rodríguez, *Chem. Soc. Rev.* **40**, 5442–5456 (2011).
84. V. W.-W. Yam, V. K.-M. Au, and S. Y.-L. Leung, *Chem. Rev.* **115**, 7589–7728 (2015).
85. M. K. Beyer and H. Clausen-Schaumann, *Chem. Rev.* **105**, 2921–2948 (2005).
86. X. Zhang, Z. Chi, Y. Zhang, S. Liu and J. Xu, *J. Mater. Chem. C* **1**, 3376–3390 (2013).
87. Z. Chi, X. Zhang, B. Xu, X. Zhou, C. Ma, Y. Zhang, S. Liu and J. Xu, *Chem. Soc. Rev.* **41**, 3878–3896 (2012).
88. Y. Sagara and T. Kato, *Nat. Chem.* **1**, 605–610 (2009).
89. A. Pucci and G. Ruggeri, *J. Mater. Chem.* **21**, 8282–8291 (2011).
90. M. M. Caruso, D. A. Davis, Q. Shen, S. A. Odom, N. R. Sottos, S. R. White and J. S. Moore, *Chem. Rev.* **109**, 5755–5798 (2009).
91. K. Ariga, T. Mori and J. P. Hill, *Adv. Mater.* **24**, 158–176 (2012).
92. T. Tsukuda, M. Kawase, A. Dairiki, K. Matsumoto and T. Tsubomura, *Chem. Commun.* **46**, 1905–1907 (2010).
93. M. Babashkina, D. Safin, M. Bolte and Y. Garcia, *Dalton Trans.* **40**, 8523–8526 (2011).
94. S. Perruchas, X. Le Goff, S. Maron, I. Maurin, F. Guillen, A. Garcia, T. Gacoin and J. Boilot, *J. Am. Chem. Soc.* **132**, 10967–10969 (2010).
95. Q. Benito, I. Maurin, T. Cheisson, G. Nocton, A. Fargues, A. Garcia, C. Martineau, T. Gacoin, J.-P. Boilot and S. Perruchas, *Chem. Eur. J.* **21**, 5892–5897 (2015).
96. H. Bi, D. Chen, D. Li, Y. Yuan, D. Xia, Z. Zhang, H. Zhang and Y. Wang, *Chem. Commun.* **47**, 4135–4137 (2011).
97. E. Szerb, A. Talarico, I. Aiello, A. Crispini, N. Godbert, D. Pucci, T. Pugliese and M. Ghedini, *Eur. J. Inorg. Chem.* 3270–3277 (2010).

98. S. Mizukami, H. Houjou, K. Sugaya, E. Koyama, H. Tokuhisa, T. Sasaki and M. Kanesato, *Chem. Mater.* **17**, 50–56 (2005).
99. H. Ito, T. Saito, N. Oshima, N. Kitamura, S. Ishizaka, Y. Hinatsu, M. Wakeshima, M. Kato, K. Tsuge and M. Sawamura, *J. Am. Chem. Soc.* **130**, 10044–10045 (2008).
100. J. Liang, F. Hu, X. Lv, Z. Chen, Z. Chen, J. Yin, G. Yu and S. Liu, *Dyes Pigm.* **95**, 485–490 (2012).
101. J. Ni, X. Zhang, Y. Wu, L. Zhang and Z. Chen, *Chem.–Eur. J.* **17**, 1171–1183 (2011).
102. D. Genovese, A. Aliprandi, E. A. Prasetyanto, M. Mauro, M. Hirtz, H. Fuchs, Y. Fujita, H. Uji-I, S. Lededkin, M. Kappes and L. De Cola, *Adv. Funct. Mat.* **26**, 5271–5278 (2016).
103. Y. Hong, J. W. Y. Lam and B. Z. Tang, *Chem. Soc. Rev.* **40**, 5361–5388 (2011).
104. B. Xu, Z. Chi, X. Zhang, H. Li, C. Chen, S. Liu, Y. Zhang and J. Xu, *Chem. Commun.* **47**, 11080–11082 (2011).
105. G. G. Shan, H. B. Li, J. S. Qin, D. X. Zhu, Y. Liao and Z. M. Su, *Dalton Trans.* **41**, 9590–9593 (2012).
106. G. D. Scholes, G. R. Fleming, A. Olaya-Castro and R. van Grondelle, *Nat. Chem.* **3**, 763–774 (2011).
107. G. D. Scholes *Annual. Rev. Phys. Chem.* **54**, 57–87 (2003).
108. V. Sundström, T. Pullerits and R. van Grondelle, *J. Phys. Chem. B* **103**, 2327–2346 (1999).
109. Solar Fuels via Artificial Photosynthesis D. Gust, T. A. Moore and A. L. Moore, *Acc. Chem. Res.* **42**, 1890–1898 (2009).
110. M. S. Choi, T. Yamazaki, I. Yamazaki and T. Aida, *Angew. Chem. Int. Ed.* **43**, 150–158 (2004).
111. Y. Nakamura, N. Aratani and A. Osuka, *Chem. Soc. Rev.* **36**, 831–845 (2007).
112. F. M. Raymo and J. Fraser Stoddart, *Chem. Ber.* **129**, 981–990 (1996).
113. S. Speiser, *Chem. Rev.* **96**, 1953–1976 (1996).
114. L. De Cola and P. Belser, *Coord. Chem. Rev.* **177**, 301–346 (1998).
115. A. Harriman and J.-P. Sauvage, *Chem. Soc. Rev.* **25**, 41–48 (1996).
116. P. A. Tanner, L. Zhou, C. Duan and K.-L. Wong, *Chem. Soc. Rev.* **47**, 5234–5265 (2018).
117. B. N. G. Giepmans, S. R. Adams, M. H. Ellisman and R. Y. Tsien, *Science* **312**, 217–224 (2006).
118. A. J. P. Teunissen, C. Pérez-Medina, A. Meijerink and W. J. M. Mulder, *Chem. Soc. Rev.* **47**, 7027–7044 (2018).
119. L. Stryer, *Ann. Rev. Biochem.* **47**, 819–846 (1978).

120. B. Valeur, *Molecular Fluorescence: Principles and Applications*, Wiley-VCH Verlag GmbH (2001).
121. S. Tyagi and F.R. Kramer, *Nat. Biotechnol.* **14**, 303–308 (1996).
122. A. Okamoto, *Chem. Soc. Rev.* **40**, 5815–5828 (2011).
123. D. L. Dexter and J. H. Schulman, *J. Chem. Phys.* **22**, 1063–1070 (1954).
124. E. K. Kainmüller, E. P. Olle and W. Bannwarth, *Chem. Commun.* 5459–5461 (2005).
125. M.-J. Li, K. M.-C. Wong, C. Yi and V. W.-W. Yam, *Chem.-Eur. J.* **18**, 8724–8730 (2012).
126. H. Takakusa, K. Kikuchi, Y. Urano, S. Sakamoto, K. Yamaguchi and T. Nagano, *J. Am. Chem. Soc.* **124**, 1653–1657 (2002).
127. L.-S. Zhang and M. E Mummert, *Anal. Biochem.* **379**, 80–85 (2008).
128. J. Zhang, Y. Shen, S. L. May, D. C. Nelson and S. Li, *Angew. Chem., Int. Ed.* **51**, 1865–1868 (2012).
129. Y. Yan, *Curr. Opin. Chem. Biol.* **7**, 635–640 (2003).
130. I. Hemmilä and V. Laitala, *J. Fluorescence* **15**, 529–542 (2005).
131. L. E. Morrison, *Anal. Biochem.* **174**, 101–120 (1988).
132. G. Mathis, *Clin. Chem.* **39**, 1953–1959 (1993).
133. T. Heyduk and E. Heyduk *Anal. Biochem.* **289**, 60–67 (2001).
134. S. G. Jones, D. Y. Lee, J. F. Wright, J. N. Jones, M. L. Tear, S. J. Gregory, and D. D. Burns, *J. Fluorescence* **11**, 13–21 (2001).
135. D. Maurel, J. Kniazeff, G. Mathis, E. Trinquet, J. P. Pin, and H. Ansanay *Anal. Biochem.* **329**, 253–262 (2004).
136. L. Kokko, K. Sandberg, T. Lovgren, and T. Soukka, *Anal. Chim. Acta* **503**, 155–162 (2004).
137. D. L. Dexter, *J. Chem. Phys.* **21**, 836–850 (1953).
138. M. Li and P. R. Selvin, *Bioconjugate Chem.* **8**, 127–132 (1997).
139. P. R. Selvin, T. M. Rana, and J. E. Hearst, *J. Am. Chem. Soc.* **116**, 6029–6030 (1994).
140. K. Blomberg, P. Hurskainen and I. Hemmila, *Clin. Chem.* **45**, 855–861 (1999).
141. N. Hildebrandt, K. D. Wegner and W. R. Algar, *Coord. Chem. Rev.* **273–274**, 125–138 (2014).
142. J. Karvinen, P. Hurskainen, S. Gopalakrishnan, D. Burns, U. Warrior, and I. Hemmila *J. Biomol. Screen* **7**, 223–231 (2002).
143. J. Karvinen, V. Laitala, M. L. Makinen, O. Mulari, J. Tamminen, J. Hermonen, P. Hurskainen, and I. Hemmila, *Anal. Chem.* **76**, 1429–1436 (2004).

144. D. L. Earnshaw and K. J. Moore, *J. Biomol. Screen.* **4**, 239–248 (2004).
145. J. Karvinen, A. Elomaa, M. L. Makinen, H. Hakala, V. M. Mukkala, J. Peuralahti, P. Hurskainen, J. Hovinen, and I. Hemmila, *Anal. Biochem.* **325**, 317–325 (2004).
146. S. S. Skourtisa, C. Liub, P. Antonioua, A. M. Virshup and D. N. Beratan, *Proc. Natl. Acad. Sci.* **113**, 8115–8120 (2016).
147. Th. Förster, *Discuss. Faraday Soc.* **27**, 7–17 (1959).
148. F. Barigelletti and L. Flamigni, *Chem. Soc. Rev.* **29**, 1–12 (2000).
149. B. Schlicke, P. Belsler, L. De Cola, E. Sabbioni and V. Balzani, *J. Am. Chem. Soc.* **121**, 4207–4214 (1999).
150. F. Barigelletti, L. Flamigni, M. Guardigli, A. Juris, M. Beley, S. Chodorowski-Kimmes, J.-P. Collin and J.-P. Sauvage, *Inorg. Chem.* **35**, 136–142 (1996).
151. L. Hammarström, F. Barigelletti, L. Flamigni, N. Armaroli, A. Sour, J.-P. Collin and J.-P. Sauvage, *J. Am. Chem. Soc.* **118**, 11972–11973 (1996).
152. M. Isaac, S. A. Denisov, A. Roux, D. Imbert, G. Jonusauskas, N. D. McClenaghan and O. S  n  que, *Angew. Chem. Int. Ed.* **54**, 11453–11456 (2015).
153. J. A. Delmar, C.-C. Su and E. W. Yu, *Biometals* **26**, 593–607 (2013).
154. I. R. Loftin, S. Franke, N. J. Blackburn and M. M. McEvoy, *Protein Sci.* **16**, 2287–2293 (2007).
155. Y. Xue, A. V. Davis, G. Balakrishnan, J. P. Stasser, B. M. Staehlin, P. Focia, T. G. Spiro, J. E. Penner-Hahn and T. V. O’Halloran, *Nat. Chem. Biol.* **4**, 107–109 (2008).
156. H. Masuhara, H. Shioyama, T. Saito, K. Hamada, S. Yasoshima and N. Mataga, *J. Phys. Chem.* **88**, 5868–5873 (1984).
157. C. Mongin, S. Garakyaraghi, N. Razgoniaeva, M. Zamkov and F. N. Castellano, *Science* **351**, 6271, 369–371 (2016).
158. M. Amelia, A. Lavie-Cambot, N. D. McClenaghan and A. Credi, *Chem. Commun.* **47**, 325–327 (2011).
159. W. E. Ford and M. A. J. Rodgers, *J. Phys. Chem.* **96**, 2917–2920 (1992).
160. M. Hissler, A. Harriman, A. Khatyr and R. Ziessel, *Chem.–Eur. J.* **5**, 3366–3381 (1999).
161. J. A. Simon, S. L. Curry, R. H. Schmehl, T. R. Schatz, P. Piotrowiak, X. Jin and R. P. Thummel, *J. Am. Chem. Soc.* **119**, 11012–11022 (1997).
162. G. J. Wilson, A. Launikonis, W. H. F. Sasse and A. W. H. Mau, *J. Phys. Chem. A* **102**, 5150–5156 (1998).
163. X.-y. Wang, A. Del Guerzo and R. H. Schmehl, *J. Photochem. Photobiol. C* **5**, 55–77 (2004).

164. N. D. McClenaghan, Y. Leydet, B. Maubert, M. T. Indelli and S. Campagna, *Coord. Chem. Rev.* **249**, 1336–1350 (2005).
165. A. Lavie-Cambot, C. Lincheneau, M. Cantuel, Y. Leydet and N. D. McClenaghan, *Chem. Soc. Rev.* **39**, 506–515 (2010).
166. S. Denisov, S. Yu, G. Jonusauskas, J.-L. Pozzo and N. D. McClenaghan, *ChemPhysChem* **17**, 1794–1804 (2016).
167. B. Maubert, N.D. McClenaghan, M. T. Indelli and S. Campagna, *J. Phys. Chem. A* **107**, 447–455 (2003).
168. J. Solarski, G. Angulo and A. Kapturkiewicz, *J. Photochem. Photobiol. A –Chem.* **218**, 58–63 (2011).
169. J. Solarski, G. Angulo and A. Kapturkiewicz, *J. Photochem. Photobiol. A –Chem.* **274**, 73–82 (2014).
170. N. D. McClenaghan, F. Barigelletti, B. Maubert and S. Campagna, *Chem. Commun.* 602–603 (2002).
171. D. S. Tyson and F. N. Castellano, *J. Phys. Chem. A* **103**, 10955 (1999).
172. H. Hofmeiera and U. S. Schubert, *Chem. Soc. Rev.* **33**, 373–399 (2004).
173. S. Campagna, F. Puntoriero, F. Nastasi, G. Bergamini and V. Balzani. In In: Balzani V., Campagna S. (eds) *Photochemistry and Photophysics of Coordination Compounds I*, vol 280, pp 117–214, *Top. Curr. Chem.*, Springer, Berlin (2007).
174. Y.-Q. Fang, N. J. Taylor, F. Laverdière, G. S. Hanan, F. Loiseau, F. Nastasi, S. Campagna, H. Nierengarten, E. Leize-Wagner and A. Van Dorsselaer, *Inorg. Chem.* **46**, 2854–2863 (2007).
175. R. Passalacqua, F. Loiseau, S. Campagna, Y.-Q. Fang and G. S. Hanan, *Angew. Chem., Int. Ed.* **42**, 1608–1611 (2003).
176. M. Abrahamsson, M. Jager, R. J. Kumar, T. Osterman, P. Persson, H.-C. Becker, O. Johansson and L. Hammarström, *J. Am. Chem. Soc.* **130**, 15533–15542 (2008).
177. G. Ragazzon, P. Verwilt, S. A. Denisov, A. Credi, G. Jonusauskas and N. D. McClenaghan, *Chem. Commun.*, **49**, 9110–9112 (2013).
178. S. A. Denisov, Q. Gan, X. Wang, L. Scarpantonio, Y. Ferrand, B. Kauffmann, G. Jonusauskas, I. Huc, and N. D. McClenaghan *Angew. Chem. Int. Ed.*, **55**, 1328–1333 (2016).
179. A. F. Morales, G. Accorsi, N. Armaroli, F. Barigelletti, S. J. A. Pope and M. D. Ward, *Inorg. Chem.* **41**, 6711–6719 (2002).
180. C. Kerzig and O. S. Wenger, *Chem. Sci.* **9**, 6670–6678 (2018).

181. T. N. Singh-Rachford and F. N. Castellano, *Coord. Chem. Rev.* **254** 21-22, 2560-2573 (2010).
182. C. Mongin, P. Moroz, M. Zamkov and F. N. Castellano, *Nat. Chem.* **10**, 225-230 (2018).
183. M. La Rosa, S. A. Denisov, G. Jonusauskas, N. D. McClenaghan and A. Credi, *Angew. Chem. Int. Ed.* **57**, 3104–3107 (2018).
184. Z. Yang, Z. Mao, Z. Xie, Y. Zhang, S. Liu, J. Zhao, J. Xu, Z. Chi and M. P. Aldred, *Chem. Soc. Rev.* **46**, 915-1016 (2017).
185. R. Czerwieniec, J. Yu and H. Yersin, *Inorg. Chem.* **50**, 8293–8301 (2011).
186. A. Lavie-Cambot, M. Cantuel, Y. Leydet, G. Jonusauskas, D. M. Bassani and N. D. McClenaghan, *Coord. Chem. Rev.* **252**, 2572–2584 (2008).
187. H. B. Gray and J. R. Winkler, *Proc. Natl. Acad. Sci.* **102**, 3534–3539 (2005).
188. M. A. Fox and M. Chanon, *Photoinduced Electron Transfer Part A: Conceptual Basis*, Elsevier, Amsterdam (1988).
189. V. Balzani, *Electron Transfer in Chemistry*, Wiley-VCH, Weinheim (2001).
190. S. Y. Reece and D. G. Nocera, *Annu. Rev. Biochem.* **78**, 673–699 (2009).
191. M. Natali, S. Campagna and F. Scandola, *Chem. Soc. Rev.* **43**, 4005–4018 (2014).
192. H. Oevering, M. N. Paddon-Row, H. Heppener, A. M. Oliver, E. Cotsaris, J. W. Verhoeven and N. S. Hush, *J. Am. Chem. Soc.* **109**, 3258–3269 (1987).
193. M. N. Paddon-Row, A. M. Oliver, J. M. Warman, K. Y. Smit, M. P. De Haas, H. Oevering and J. W. Verhoeven, *J. Chem. Phys.*, **92**, 6958–6967 (1988).
194. A. M. Oliver, D. C. Craig, M. N. Paddon-Row, J. Kroon and J. W. Verhoeven, *Chem. Phys. Lett.* **150**, 366–373 (1988).
195. J. M. Lawson, D. C. Craig, M. N. Paddon-Row, J. Kroon and J. W. Verhoeven, *Chem. Phys. Lett.* **164**, 120–125 (1989).
196. M. R. Wasielewski, M. P. Niemczyk, W. A. Svec and E. B. Pewitt, *J. Am. Chem. Soc.* **107**, 5562–5563 (1985).
197. J. P. Collin, S. Guillerez and J.-P. Sauvage, *J. Chem. Soc., Chem. Commun.* 776–778 (1989).
198. J. P. Collin, S. Guillerez, J.-P. Sauvage, F. Barigelletti, L. De Cola, L. Flamigni and V. Balzani, *Inorg. Chem.* **30**, 4230–4238 (1991).
199. R. Hoffman, A. Inamura and W. J. Here, *J. Am. Chem. Soc.* **90**, 1499–1509 (1968).
200. M. N. Paddon-Row, A. M. Oliver, M. C. R. Symons, E. Cotsaris, S. S. Wong and J. W. Verhoeven. In Hall, D.O.; Grassi, G. Eds., *Photoconversion Processes for Energy and Chemicals*, p. 79, Elsevier, Amsterdam (1989).

201. D. Rehm and A. Weller, *Isr. J. Chem.* **8**, 259–271 (1970).
202. B. Song, G. L. Wang, M. Q. Tan and J. L. Yuan, *J. Am. Chem. Soc.* **128**, 13442–13450 (2006).
203. C. Mathonière, *Eur. J. Inorg. Chem.* 248–258 (2018).
204. D. Aguila, Y. Pardo, E. Koumoussi, C. Mathonière and R. Clérac, *Chem. Soc. Rev.* **45**, 203–224 (2016).
205. A. Bleuzen, V. Marvaud, C. Mathonière, B. Sieklucka and M. Verdaguer, *Inorg. Chem.* **48**, 3453–3466 (2009).
206. S.-i. Ohkoshi and H. Tokoro, *Acc. Chem. Res.* **45**, 1749–1758 (2012).
207. N. Shimamoto, S.-i. Ohkoshi, O. Sato and K. Hashimoto, *Inorg. Chem.* **41**, 678–684 (2002).
208. Y. Zhang, D. Li, R. Clérac, M. Kalisz, C. Mathonière and S. M. Holmes, *Angew. Chem., Int. Ed.* **49**, 3752–3756 (2010).
209. D. M. D’Alessandro and F. R. Keene, *Chem. Rev.* **106**, 2270–2298 (2006).
210. S. Silvi and A. Credi, *Chem. Soc. Rev.* **44**, 4275–4289 (2015).
211. J. Crassous, *Chem. Commun.* **48**, 9684–9692 (2012).
212. J. Crassous, *Chem. Soc. Rev.* **38**, 830–845 (2009).